T cell response to intact SARS-CoV-2 includes coronavirus cross-reactive and variant-specific components

Lichen Jing [1,*]

Xia Wu [1,*]

Maxwell P. Krist [1,*]

Tien-Ying Hsiang [2]

Victoria L. Campbell [1]

Christopher L. McClurkan [1]

Sydney M. Favors [1]

Lawrence A. Hemingway [1]

Charmie Godornes [1]

Denise Q. Tong [1]

Stacy Selke [3]

Angela C. LeClair [1]

Chu-Woo Pyo [7]

Daniel E. Geraghty [7]

Kerry J. Laing [1]

Anna Wald [1, 3, 6, 8]

Michael Gale Jr. [2, 4, 5]

David M. Koelle [1, 3, 5, 8, 9, 10]

[*] Contributed equally

[1] Department of Medicine, University of Washington

[2] Department of Immunology, University of Washington

[3] Department of Laboratory Medicine and Pathology, University of Washington

[4] Center for Innate Immunity of Immune Disease, Department of Immunology, University of Washington

[5] Department of Global Health, University of Washington

[6] Department of Epidemiology, University of Washington

[7] Clinical Research Division, Fred Hutchinson Cancer Research Center

[8] Vaccine and Infectious Diseases Division, Fred Hutchinson Cancer Research Center

[9] Benaroya Research Institute, Seattle

[10] Correspondence: David Koelle, 750 Republican Street, Room E651, Seattle, WA, 98109, 206 616 1940, dkoelle@medicine.washington.edu

Funding

NIH contract HHSN75N93019C00063 (DMK) and HHSN272201600027C (DEG), and NIH grants AI163999 (DMK, XW), and AI118916, AI104002, and AI115296 (MG).

Acknowledgements

We thank the participants, the University of Washington Virology Research Clinic and Immunology Cell Analysis Facility, the Flow Core at Seattle Children's Research Institute, Jesse Bloom, Katharine Crawford, Keara Malone, Andrea Loes, and Allison Greaney for SARS-CoV-2 plasmids, Ralph Baric for Vero-E6-USAMRIID cells and SARS-CoV-2-strain WA1-GFP, and Thomas Snyder and Adaptive Biotechnologies for Immunoseq™ sequencing.

Author Contributions

Conceptualization: DMK, LJ, XW; Data curation and bioinformatic analysis: XW, LJ, MPK, DMK; Funding acquisition: MG, DEG, DMK; Investigation: LJ, XW, MPK, VLC, T-YH, CLM, C-WP, SMF, LH, CG, DT, KJL, DG; Data management: SS; Clinical protocol: AW, ACL; Supervision: DMK, MG; Writing: DMK, XW, MPK, LJ, KL.

Abstract

SARS-CoV-2 provokes a brisk T cell response. Peptide-based studies exclude antigen processing and presentation biology and may influence T cell detection studies. To focus on responses to whole virus and complex antigens, we used intact SARS-CoV-2 and full-length proteins with DC to activate CD8 and CD4 T cells from convalescent persons. T cell receptor (TCR) sequencing showed partial repertoire preservation after expansion. Resultant CD8 T cells recognize SARS-CoV-2-infected respiratory cells, and CD4 T cells detect inactivated whole viral antigen. Specificity scans with proteome-covering protein/peptide arrays show that CD8 T cells are oligospecific per subject and that CD4 T cell breadth is higher. Some CD4 T cell lines enriched using SARS-CoV-2 cross-recognize whole seasonal coronavirus (sCoV) antigens, with protein, peptide, and HLA restriction validation. Conversely, recognition of some epitopes is eliminated for SARS-CoV-2 variants, including spike (S) epitopes in the alpha, beta, gamma, and delta variant lineages.

Introduction

The acquired immune response to SARS-CoV-2 can limit infection, as shown by protection from re-infection (1) and the efficacy of vaccines (2). While antibodies can prevent infection and disease, T cell depletion studies of convalescent or vaccinated animals strongly suggest active roles for T cells (3). Many studies have defined regions of the predicted SARS-CoV-2 proteome that can activate T cells in blood (4, 5). This work typically uses single or pooled peptides, or peptide-based reagents such as HLA multimers. Some workflows result in cell death that limit follow-up, while others, such as activation-induced marker (AIM)-based cell sorting (6) allow recovery of live cells for downstream work. Taken together, peptide-based studies provide a large thesaurus of reactive peptides, and in some cases, relevant HLA restricting alleles and TCR sequences. However, validation of reactivity with whole virus or complex antigens is less frequently reported.

The present report used PBMC from a cohort of coronavirus-19 (COVID-19) convalescent persons (7-10) to begin to study T-cell responses to SARS-CoV-2 in the contexts of direct- and cross-presentation of complex viral antigens. Validation with proteome-covering full-length protein and peptide sets allowed definition and confirmation of many individual epitopes. Expanded responder cell populations also permit detailed study of HLA restriction, functional avidity, cross-recognition of sCoV, and recognition of circulating SARS-CoV-2 variants including variants being monitored (VBM) and variants of concern (VOC).

Estimates of the overall magnitude of the CD4 and CD8 T cell response to SARS-CoV-2, as a percent of circulating PBMC at times soon after clinical recovery are around the 0.5-1% level based on the summation of peptide reactivities (4, 11, 12). We were interested in benchmarking peptide-based estimates for SARS-CoV-2 to the levels of reactivity to whole viral antigen, and in

comparing epitope specificities determined using peptide sets and more complex antigens. It is well established that T cell clonotypes show cross-reactivity to unrelated peptide epitopes presented by a single HLA allele, for example cross-recognition of disparate influenza and EBV peptides with HLA A*02:01 (13), pathogenic cross-recognition of influenza and self-epitopes (14), and potentially beneficial cross-reactivity between viruses and tumor antigens (15). The same TCR can also recognize peptides presented by divergent HLA alleles, for example the alloreactivity of herpes simplex virus (HSV)- or EBV-specific T cells against HLA-mismatched antigen presenting cells (APC) bearing endogenous peptides (16, 17). Reactivities detected solely using SARS-CoV-2 peptide sets could include such cross-reactivity. The use of complex SARS-CoV-2 antigens to enrich responses also incorporates antigen processing and presentation steps, such as proteosomal cleavage, peptide transport into the endoplasmic reticulum and trimming during HLA loading, that can be influenced by flanking sequences within proteins, as well as potentially incorporating post-translational modifications and cryptic ORFs absent from peptide sets (18, 19). We also studied recognition of whole SARS-CoV-2 at the effector stage: CD8 T cell assays used infected bronchial epithelial cells HLA-matched to CD8 effector T cells, while CD4 T cell readouts used SARS-CoV-2 antigen and appropriate APC. Importantly, we also checked if T cells enriched using simpler peptide or protein antigens could recognize whole virus.

SARS-CoV-2 shares genomic structure and sequence motifs with sCoV. Cross-reactivity with sCoV has been described (20) but is less studied in the whole virus context. SARS-CoV-2 also shows modest sequence variation, and variants and deletions emerge within-subject in immune suppressed persons (21), and within populations (22). In the present report, we use culture-amplified T cell responders to probe recognition of sCoV and variant SARS-CoV-2 T cell epitopes.

Results

Subjects and specimens. We studied 26 specimens from 12 subjects (Supplementary Table 1) with COVID-19 in March or April 2020, prior to detection of VOCs in the study region (23). Each subject reported SARS-CoV-2 RNA detection, positive serum or plasma anti-S domain 1 and anti-N IgG, and SARS-CoV-2 neutralizing antibody (nAb) titer $\geq$ 1:40 (7). Median age was 56 (range 32 to 72) and sex was balanced. Amongst 4 hospitalized subjects, 3 required intensive care. Median illness duration was 16 days (range 4 to 32). PBMC were obtained a median of 138 days after recovery (range 31 to 256). We used several methods to enrich SARS-CoV-2-specific T cells for detailed studies (outlined in Supplementary Fig. 1).

PBMC T cell responses to whole SARS-CoV-2 antigen. SARS-CoV-2 WA1 antigen was prepared from infected cells, rather than from purified virions, to include non-structural proteins (NSPs) (24). We used dual expression of CD137 and CD69 for analytic AIM and to sort cells for expansion (Fig. 1) (25). We observed a median of 0.16% (range 0.089% to 0.33%) of CD4 T cells were AIM (+) (n=5, Supplementary Table 2). Responses to mock antigen were low (median 0.026%, range 0.009%-0.061%). Responses to viral antigen were higher than to mock antigen ($p = 0.0078$ by pair-wise analysis); the median net response was 0.13%. Absolute and net responses to whole SARS-CoV-2 antigen in HD PBMC were low, with no significant net virus-specific signal (Supplementary Fig. 2B). We sorted a median of 389 AIM (+) CD4 T cells (machine counts, range 375 - 2,138) per specimen from the 5 COVID-19 convalescent subjects (Supplementary Table 2).

After expansion with a generalized mitogenesis protocol, T cell line (TCL) functional enrichment was measured as reactivity to whole killed SARS-CoV-2. Autologous PBMC used as APC were dump-gated and IFN-γ and IL-2 expression used to enumerate SARS-CoV-2-specific CD4 T

cells (8, 11). We observed robust TCL enrichment of virus-reactive CD4 T cells. For example, participant W003 TCL had net 8.14% of cells responding to whole SARS-CoV-2 (Fig. 1C), a 61-fold enrichment over the PBMC CD4 T cell AIM signal. Enrichment ranged from 41- to 201-fold for the 5 subjects (Supplementary Table 2).

Both monocytes in fresh PBMC and moDC can process and present antigens to CD4 T cells. Higher levels of PBMC CD4 T cell activation were noted when autologous DC were used as initial APC (Fig. 1B) compared to direct addition of killed virus to PBMC. Background signal for mock antigen also slightly increased (median 0.16%, range 0.11%-0.47%). The median net proportion of AIM (+) CD4 T cells was 0.66% (range 0.35% to 2.43%) across 12 samples. Use of moDC allowed the sorting of a median of 11,320 activated CD4 T cells per specimen (range 8,190 to 19,860), from which 20% were culture-expanded (Supplementary Table 2) and 80% used for *ex vivo* TCR sequencing.

In addition to presentation to CD4 T cells, moDC can cross-present inactivated antigen to CD8 T cells. Using moDC, we observed specific CD8 T cell activation as measured by CD69 and CD137 co-expression (Fig. 1B). Negative control antigen was immunologically silent. We did not detect PBMC CD8 T cell responses in HD (Supplementary Fig. 2). As with CD4 T cells, higher net proportions of AIM (+) CD8 T cells were noted with moDC (n = 12, median 0.95%, range 0.27 to 1.62%) than without (n = 5, median 0.033%, range 0.013%-0.29%) (Supplementary Fig. 2B, Supplementary Table 2). A median of 842 CD8 T cells (range, 411 - 2,611) were expanded per specimen, while 80% of the AIM-sorted cell populations were TCR-sequenced.

Two subjects were studied using moDC at five time points each between 32 to 256 days after recovery from COVID-19. Decreasing CD4 and CD8 AIM (+) abundance was noted over time (Supplementary Table 2). Subject W005 had consistently higher CD4 than CD8 T cell

responses, with the ratio of activated cells ranging from 1.54 to 3.15. A reciprocal pattern was seen in subject W012, with consistent CD4/CD8 ratios of AIM (+) cells < 1.

TCR repertoire tracking during T cell expansion. We used the moDC workflow to present whole SARS-CoV-2 antigen (above), and analyzed AIM (+) CD4 and CD8 T cells from three subjects at two time points each. A portion of AIM (+) cells were directly sequenced, and a portion sequenced after expansion, with a genomic DNA-based method (26). A median of 6.75% of CDR3 aa sequences detected *ex vivo* were found in expanded cultures. Reciprocally, a median of 16.75% of productive CDR3 aa sequences in the expanded cultures were detected in the corresponding ex vivo samples (representative data, Supplementary Fig. 3A). CDR3 abundances showed excellent agreement for AIM (+) cells after one vs two expansions (representative data, Supplementary Fig. 3B). A possible factor contributing to repertoire differences *ex vivo* vs. post-expansion is poor recovery of DNA from small *ex vivo* specimens. Amongst the 12 *ex vivo* samples, the median number of productive CDR3 gene rearrangements reported was 11.6% (range, 4.9-21.7%) of the sorting cell counts.

Alternative generation of polyclonal SARS-CoV-2-reactive T cells. As an alternative approach to retains an antigen processing requirement, SARS-CoV-2 proteins were expressed in COS-7 or HeLa cells. These were harvested, inactivated, and added to PBMC without (COS-7) or with (HeLa) autologous moDC. Small increments in AIM-positive CD4 or CD8 T cells were detectable compared to mock antigen (representative data, Supplementary Fig. 4A). Finally, CD8 or CD4 T cells proliferating (representative data, Supplementary Fig. 5A) to SARS-CoV-2 peptide pools were sorted and expanded.

CD8 T cell recognition of infected cells. CD8 T cell recognition typically requires HLA matching. HBEC3-KT-A are permissive for SARS-CoV-2 replication and are HLA A*03:01 (+)

(Supplementary Table 3). For effector CD8 T cells we stimulated PBMC from HLA A*03:01 (+) participant W003 with autologous DC loaded with S protein-expressing HeLa cells, sorted AIM (+) CD8 T cells, expanded them, and showed they recognized S protein in the HLA A*03:01 context (Supplementary Fig. 6A). A reactive peptide, S 377-389, was found using peptide matrices (Supplementary Fig. 6B) containing the HLA A*03:01-restricted epitope S 378-386 (27). A fluorescent A*03:01-S 378-386 tetramer allowed further enrichment of CD8 T cells (Supplementary Fig. 6C). We then examined if S protein could be processed and presented by virus-infected cells. CD8 T cells specifically recognized SARS-CoV-2-infected HBEC3-KT-A cells (Fig. 2A). Specificity control HLA A*03:01-restricted, tetramer-enriched CD8 T cells, specific for an unrelated polyomavirus epitope in MCPyV (28), were active when tested with polyomavirus peptide-pulsed HBEC3-KT-A positive controls (Fig. 2B) but did not recognize SARS-CoV-2-infected target cells (Fig. 2A).

CD8 T cell responses to full-length SARS-CoV-2 proteins. CD8 T cell target diversity was studied using whole virus stimulation followed by SARS-CoV-2 proteome-wide scans using subject-specific HLA A and B aAPC panels. A complex response was observed for subject W005, hospitalized in the ICU and studied 32 days after recovery, by incorporating DC boosting. This subject had an HLA B*15:02-restricted response to NSP2, HLA A*11:01- and B*15:02-restricted responses to nucleoprotein, and an HLA B*51:01-restricted response to ORF3A (Fig. 3A). Multiple proteins were positive for subject W012, while subject W001, studied using moDC, only showed responses to ORF9B (summarized in Fig. 4A). Even when moDC were not used, the aAPC-proteome panels were successful for bulk AIM-enriched CD8 TCL enriched with whole virus. For example, subject W010 had a single HLA A*01:01-restricted response detected for NSP3 (Fig. 3B). This was confirmed at the peptide level (Fig. 3C), allowing tetramer enrichment (Fig. 3D) and use of tetramer-enriched cells confirmed as ORF- and peptide-reactive (Fig. 3E) to determine functional avidity (Fig. 3F).

CD4 T cell responses to full-length SARS-CoV-2 proteins. AIM-sorted, expanded CD4 TCL, enriched with or without DC boosting, were similarly tested proteome-wide. Each SARS-CoV-2 ORF or cleaved polypeptide product of ORFs polypeptide (PP)1a and PP1ab(29) was expressed (30). Readout assays included Th1 cytokine ICS (supplementary Fig. 7A), proliferation (supplementary Fig. 7B), and IFN-γ secretion (supplementary Fig. 7C). Across 17 specimens from 8 persons, a median of 7 proteins were recognized per specimen (range, 3 to 15) (summarized in Fig. 4B). The SARS-CoV-2 proteins recognized in the highest percentage of participants were S, membrane (M), nucleoprotein (N), and ORF9B (Fig. 4B). Reactivity to ORF3A, ORF7A, NSP2, and NSP3 were also noted in 50% or more of participants. Because DC were not used for all specimens and few participants were studied, conclusions about antigen breadth and dominance remain preliminary. We noted that over time, most within-participant protein-level responses were consistent. For example, participant W005 recognized NSP2, NSP13, and NSP16 at almost all time points (Fig. 4B).

CD8 T cell epitopes. TCL initiated with diverse workflows (Supplementary Fig. 1) were used. moDC-whole virus stimulation of PBMC yielded peptide epitopes (examples, Supplementary Fig. 8) to confirm ORF-level hits (Fig. 3A, Fig. 4A). PBMC stimulation with SARS-CoV-2 proteins with DC, followed by AIM sorting also yielded cultures that reacted with the relevant ORF and discrete peptides (example, Supplementary Fig. 4A, 4B), as did PBMC stimulation with pooled peptides followed by sorting of proliferated cells (Supplementary Fig. 5A, Supplementary Fig. 4C). Overall, integrated across CD8 TCL and eliminating redundancies, CD8 T cells reactive with 25 SARS-CoV-2 epitopes in the context of 8 HLA class I alleles were obtained (Supplementary Table 4).

CD4 T cell epitopes. TCL initiated with several workflows were tested to define peptide epitopes. Importantly, when TCL were started with peptide pools (as in Supplementary Fig. 5A), the resultant TCL recognized whole virus lysate and full-length protein (Supplementary Fig. 5B) as well as peptides (Supplementary Fig. 5C), suggesting epitopes discovered with peptides are relevant to viral infection. IFN-γ and proliferation readouts corresponded (representative data, Supplementary Fig. 9) and we summarize epitopes defined with either ror both readouts. Cultures initiated with complex antigen, such as from participant W001 using moDC-assisted stimulation with whole virus, yielded multiple reactive peptides (representative data, Supplementary Fig. 10). Overall, CD4 T cell epitopes were detected in 13 SARS-CoV-2 proteins. Responses were diverse within-person. For specimen 1 from participant W001 (Supplementary Table 1), 55 epitopes were confirmed in 7 proteins, including 27 epitopes in S, 7 each in N and NSP3, 6 in ORF3A, 5 in M, 2 in ORF9B, and 1 in ORF7A (Supplementary Table 5). Similarly, in participant W005 studied one month after recovery, 65 CD4 T cell epitopes were identified in 10 proteins. Altogether, we observed 240 CD4 T cell peptide reactivities from 8 persons (Supplementary Table 5). These correspond to 172 unique SARS-CoV-2 peptides (Supplementary Table 5). Amongst these, we found 70 epitopes in S protein, 26 in N protein, and 23 in M protein, with fewer in ORFs 3A, 7A, 8, and 9, and NSPs 1, 2, 3, 4, 6, and 7. Peptides with CD4 T cell recognition by at least half the population studied included M 69-81, M 177-189, S aa 133-145, S 165-177, N 289-301, and N 349-361.

CD4 T cell HLA restriction and functional avidity. Studies of CD4 T cell HLA restriction and estimated functional avidity (representative data, Supplementary Fig. 11) yielded HLA locus-level data on 118 of 123 (96%) peptides tested. Amongst these, 84 (72%) were HLA DR-restricted, 23 (20%) were HLA DQ-restricted, and 11 (8%) were HLA DP-restricted (Supplementary Table 5). HLA restriction at the locus level was generally identical if two participants recognized the same peptide, but there were exceptions. S protein aa 165-177 was

HLA DP-restricted in 4 participants and HLA DR-restricted in 2. Allele-level restriction was determined using aAPC (representative data, Supplementary Fig. 11A, 11B). We observed presentation by 10 distinct HLA DRB1, DRB3, and DRB4 alleles (Supplementary Table 5). Some peptides in SARS-CoV-2 S, M, and N proteins were presented by both DRB1 and either DRB3 or DRB4 (representative data, Supplementary Fig. 11C) or dual DRB3 alleles (not shown). Functional avidity data were available for 124 CD4 T cell epitopes (representative data, Supplementary Fig. 11, summarized in Supplemental Table 5). Responses at 1 and 10 ng/ml peptide were noted for 4 and 10 epitopes, respectively. S 165-177 was particularly potent, with responses at 1 or 10 ng/ml for 5 of 6 subjects.

Recognition of seasonal coronaviruses. Cross-recognition of SARS-CoV-2 and sCoV peptide has been documented (6, 20), but less is known about recognition of complex viral antigens. We found that polyclonal CD4 TCL each of three subjects studied, enriched from PBMC using whole SARS-CoV-2 antigen and moDC, cross-recognized either whole OC43 or whole 229E cell-associated virus (Fig. 5A). Control mock-infected virus preparations were negative. An additional CD4 TCL enriched using whole SARS-CoV-2 antigen without moDC also cross-recognized OC43. For subject W001, S proteins from both viruses were both antigenic (Fig. 5B), as were both homologs of a peptide in S. The HLA restricting allele was established as HLA DRB1*15:01 (Fig. 5C). Cross-recognition of an HLA DP-restricted peptide that is nearly identical in SARS-CoV-2, OC43, and HKU1 N proteins was also observed (Supplementary Fig. 12).

Recognition of SARS-CoV-2 variants. To choose variants for study we correlated SARS-CoV-2 T cell epitopes detected using Wu-1/WA1 reagents with variants both in early 2020 data and in early 2021 VBM, concentrating on the B.1.1.7, B.1.351, and P1 lineages. Polyclonal CD8 TCL were recovered from subject W004 using an S peptide pool (Supplementary Fig. 5A).

306 Potent recognition of strain Wu-1 peptides 269-277 YLQ and 417-425 KIA, HLA A*02:01-
307 restricted epitopes (27), was observed (Fig. 6). There was no recognition of variants with
308 substitutions K417N and K417T which are present in the B.1.351 and P.1 lineages, respectively.
309 Epitope-specific T cells enriched with tetramers (Supplementary Fig. 13A) detected full-length S
310 processed by HLA A*02:01-transfected aAPC (Supplementary Fig. 13B), but failed to recognize
311 S K417T or the full-length SARS-CoV-2 S variant from lineage B.1.351 bearing K417T.
312 Responses to S from B.1.1.7, which does not have an aa417 substitution, were intact. Control
313 CD8 T cells specific for S aa 269-277 YLQ, unchanged in these variants, were not affected
314 (Supplementary Fig. 13B). We also observed loss of CD8 TCL reactivity to SARS-CoV-2 S
315 F490S in the HLA A*29:02-restricted aa 489-497 epitope, to S K378N in the HLA A*03:01-
316 restricted aa 378-386 epitope, and to M (membrane) T175M in the HLA A*11:01 aa 169-181
317 epitope (Supplementary Fig. 13, summarized in Table 1).
318
319 Variant changes could also influence CD4 T cell recognition (primary data, Supplementary Figs.
320 14-17). In addition to loss of recognition of variant aa in B.1.1.7 (effects summarized in Table 1
321 and Fig. 7) and/or P.1 lineages, we also noted strain-specific recognition of B.1.1.7-associated
322 sequences that were already prevalent in early 2020 and not unique to VBM (example,
323 Supplementary Fig. 10, indicated in blue). A graphical summary of variants evaluated in S (Fig.
324 7) shows a mixture of responses that are either preserved, partially reduced in dose-response
325 assays, or abrogated when tested with variant peptides.

Discussion

The T cell response to SARS-CoV-2 is functionally important (31). Studies have correlated T cell kinetics, magnitude or phenotypes with disease in apparently immune competent persons with delayed or dis-coordinated immunity and poor clinical outcome (8, 32). T cell responses have been linked to protection from re-infection (33). Disease states and iatrogenic treatments that decrease T cell responses can prolong live virus shedding (34, 35). Cooperation between T and B cells, such as antigen-specific CD4 T_{FH} (36), also suggest that T cells are involved in pathogen control. Supporting this, S-specific CD4 T cell TCR breadth and depth correlate with nAb titers in COVID-19 convalescent persons (9). CD8 T cell depletion data in non-human primates indicate that these effectors contribute to vaccine-induced protection (3).

Many groups have detected responses to SARS-CoV-2 epitopes using peptide-based technologies (31), but less work has focused on T cell reactivity to complex antigens such as whole virus or full-length proteins. Both T cell priming, and effector responses of memory T cells, occur *in vivo* in the context of viral infection and/or loading of antigen into various APC, with important differences for HLA class I and II (37). In the present report, we leveraged the ability of moDC to cross-present whole viral antigen to CD8 T cells, and to present viral antigen to CD4 T cells, to enrich polyclonal SARS-CoV-2-specific T cells. Similar studies are rare; in one report, live virus induced subtle IFN-γ expression in convalescent T cells, but confirmation of virus specificity was not documented (38). Using established (25, 30, 39-42) readout methods, TCL created after whole virus or simpler antigen stimulation were used to study the breadth and specificity of the T cell response, reactivity to virus-infected cells, and recognition of sCoV and SARS-CoV-2 variants.

Acute COVID-19 most severely effects the respiratory tract, and while autopsy surveys can detect virus body-wide (43), it is likely that T cell contributions to host defense and possibly to inflammatory damage occur mostly in the respiratory tract and draining lymph nodes. Cytotoxic T cells have the potential to kill SARS-CoV-2 infected cells and thus reduce viral progeny and further cell infection. To date, reports of the ability of T cells to recognize SARS-CoV-2 infected cells are limited. We have begun such studies using the HBEC3-KT-A. We previously showed that HBEC3-KT-A cells are permissive for expression of SARS-CoV-2 ORF6 protein after infection, (44) and that infected cells stain positively for S protein and viral RNA (45). We find that HLA-matched S-specific CD8 T cells recognize virally infected cells. HBEC3-KT cells can differentiate into ciliated and mucus-producing goblet cells *in vitro* (46), and *in vivo*, ciliated respiratory epithelial cells have the highest levels of SARS-CoV-2 RNA (47). Zhang *et al.* have reported that the SARS-CoV-2 ORF8 protein can down-regulate HLA class I and limit CD8 T cell killing of peptide-sensitized target cells (48). Wagner *et al.* have shown recognition of SARS-CoV-2-infected cancer-origin lung alveolar cells by overexpressing ACE2 and exogenous HLA class I alleles. Effector cells were allogeneic T cells engineered to express TCRs specific for SARs-CoV-2 (49). Many viruses encode CD8 T cell evasion functions, effects that can be selective for non-transformed, physiologically relevant APC (50). We are currently optimizing SARS-CoV-2 infection of primary human nasal epithelial cells, differentiated to ciliated and goblet phenotypes, and pursuing CD8 recognition studies of other SARS-CoV-2 proteins, target cell killing, and reduction of viral yield in CD8 T cell studies.

A cytotoxic CD4 T cell phenotype has been detected during acute SARS-CoV-2 infection (51, 52). Upper and lower respiratory tract epithelial cells can display HLA class II required for CD4 T cell recognition, and pulmonary alveolar macrophages are excellent APC for CD4 T cells and are abundant in COVID-19 pneumonia, containing SARS-CoV-2 antigen (53). Thus, CD4 T cell

recognition of whole viral antigen could be relevant to lung infection, again with either salutary or damaging effects.

We studied T cell responses from relatively few persons and have not attempted to evaluate novelty per-epitope given the plethora of work in this area. Coverage of the entire viral proteome may, however, enable some novel insights. Mass spectroscopy suggests a large spectrum in SARS-CoV-2 NSP abundance in infected cell cultures (54, 55) and *in vivo* (56, 57). Previous studies suggesting that viral protein abundance is associated with CD4 T cell immunodominance (39, 58) are supported by our finding of prevalent and poly-specific responses to the abundant S and N proteins. The high population prevalence of CD4 responses to M, NSP3 and ORF3A also agree with prior work (31). We also found responses to NSP2 and ORF9B in at least half the subjects studied proteome-wide. NSP2 has previously been described as a CD4 immunogen in convalescent persons, while ORF9B was not included in some previous surveys (4, 11, 59-62). ORF9B is an alternative open reading frame within the nucleoprotein locus encoding a 98 aa-long ORF9B protein that is abundant in infected cells (54), localizes to mitochondria (63), elicits strong antibody responses (64), and is involved in evasion of type I IFN responses (65). CD4 T cell breadth was studied in 17 samples from 8 persons. We found a median CD4 breadth of 7 viral antigens/specimen, and that 6 of 8 persons recognized 7 or more proteins. In contrast, a survey of 99 convalescent persons with proteome-wide peptides and an *ex vivo* AIM approach found an average of 3.2 CD4 T cell antigenic proteins per person with no subject recognizing over 6 proteins (4).

TCL allowed tests of a large number of SARS-CoV-2 variant peptides. We found many examples of abrogation or reduction of recognition of variants, some from variants of concern. The literature consensus is that T cell responses to infection or vaccination are poly-specific, such that failed variant epitope recognition may not have a net deleterious effect on immunity

(31). However, detailed investigations remain warranted. Tarke *et al.* tested PBMC from convalescent persons infected early in the pandemic (66). While *ex vivo* T cell responses in convalescent PBMC measured by AIM did not differ between ancestral- and variant-derived peptide pools for CD4 or CD8 T cells, IFN-γ ELISPOT detected decreased overall for VOC compared to Wu-1 peptides. Agerer *et al.* focused the HLA A*02:01-restricted response to the S aa 269-277 YLQ epitope (67). The L270F variant showed decreased binding to HLA A*02:01 and no activation of YLQ-specific CD8 T cells. L270F has been detected in 3 of > 1.4 million global sequences. In contrast, the P272L variant we investigated has been noted over 9000 times. aa 272 is modeled to face TCR (68) and to not reduce HLA A*02:01 binding. Based on structural models (68) and other epitope variants (69, 70), the S P272L (epitope position 4) and K417N or K417T (epitope position 1) variants studied herein could generate variant-specific T cells, a hypothesis testable in convalescent PBMC. Recently, de Silva et al. documented additional examples of strain-specific CD8 T cell recognition of SARS-CoV-2 variants (71). COVID-19 vaccines mostly use Wu-1-like S antigen, such that vaccinee T cells may also detect variant-specific T cell recognition. Recently, Keeton et al. detected modest differences in CD8 T cell recognition of S between vaccine strain and delta variant peptides (72). In another vaccine study (66), AIM responses to the B.1.351 S pool were lower for CD4 and CD8 T-cells compared to Wu-1 peptides. The precise epitope and HLA restriction information in this report can focus studies of variant recognition in cases of breakthrough infection as the pandemic continues to evolve, and as epitope-based (NCT04776317) and variant-based vaccines (73) are studied in clinical trials.

The present report also adds to the growing body of literature concerning cross-recognition of sCoV and SARS-CoV-2 (20, 27, 74-76). The use of whole viral antigens in both stimulation and readout stages of our investigations of sCoV allowed us to document that polyclonal CD4 TCL from COVID-19 convalescent persons can recognize whole OC43 and 229E viral antigen. As

mentioned above, this assay format integrates antigen processing and presentation to supplement studies that focus solely on peptide reactivity. Validation to the antigen, peptide, and HLA restriction level was obtained for an epitope in OC43 S. The presence and sequencing of SARS-CoV-2 and sCoV infections in our study population are unknown. However, the timing of our specimen collection shortly after recovery from COVID-19, and sero-epidemiologic data that most adults have been infected with multiple sCoV, suggest the T cell cross-reactivities we detected may reflect prior sCoV infections boosted by SARS-CoV-2, Data concerning sCoV T cell cross-reactivity can be integrated with antibody-based (77, 78) and clinical studies (79) to determine if sCoV-specific immune memory modulate COVID-19 disease, and to guide development of possible pan-coronavirus vaccines.

The current study has limitations. We observed no AIM response to whole SARS-CoV-2 in HD, yet, several groups have documented the presence of SARS-CoV-2-reactive T cells in uninfected individuals from either the naïve or sCoV-primed memory repertoires (20, 80). Our approaches may be better suited to memory response to SARS-CoV-2 infection itself but could be adapted to capture these responses, for example by using higher input cell numbers. We noted only moderate preservation of TCR sequences comparing *ex vivo* sorted AIM (+) T cells and expanded cultures. Biological factors related to TCR repertoire differences could include rare clonotypes that assorted into either the *ex vivo* TCRseq or expansion fractions of the AIM (+) cells, rather than being represented in both. Indeed, sequencing of AIM (+) cells ex vivo shows broad and diverse responses at the TCR sequence level even to single epitopes, with many clonotypes detected at low levels (81). T cell programming could render some T cells refractory to expansion, with an exhausted T cell phenotype noted for SARS-CoV-2-specific memory T cells in some settings (82). Technical factors could also contribute, ranging from DNA extraction or PCR inefficiencies during TCR sequencing protocols to lack of provision of T cell expansion culture conditions required for some of the AIM (+) cells. Analytically, we discounted

T cell clonotypes detected at less than two copies, potentially reducing concurrency between *ex vivo* and expanded repertoires. Alternative methods such as single-cell TCRseq (83) to capture the TCR repertoire AIM (+) cells *ex vivo* can be applied in the future to study the virus-specific repertoire before and after expansion and to determine if there are transcriptional programs correlated with failure to expand. In addition, a relatively low number of persons were studied. The viral antigens used could have low abundance for some viral proteins in our antigen preparation, leading to underestimation of antigen breadth.

In conclusion, T cells are a functionally important component of the specific acquired immune response to SARS-CoV-2 infection and vaccination. We have shown brisk recognition of whole SARS-CoV-2 by both CD4 and CD8 T cells from convalescent persons, provide estimates of the integrated frequency of these cells in the circulation, and used proteome-covering tools to approach within-subject antigenic breadth at the antigen and epitope levels. We found many examples of loss of recognition of epitope variants by effector T cells recovered from persons infected early in the pandemic, and used whole viral antigens to document coronavirus cross-reactive T cell immunity.

Methods

Subjects and specimens. The COVID-19 cohort has been described (7-10). Subjects reporting SARS-CoV-2 detection and an illness compatible with COVID-19 were recruited. Subjects were seropositive for serum IgG for SARS-CoV-2 S and nucleoprotein (N) (7) (Supplementary Table 1). PBMC were cryopreserved in liquid nitrogen. Adult healthy donor (HD) PBMC were collected before 2019. Subjects provided informed written consent and studies were Institutional Review Board-approved. HLA typing was by PCR amplicon sequencing at Scisco Genetics (Seattle, WA).

Antigens. For whole viral antigen, SARS-CoV-2 strain Washington 1 (WA1) (84) (Genbank MN985325.1) was cultured on Vero-E6 USAMRIID cells (gift of Dr. Ralph Baric, University of North Carolina, Chapel Hill, NC) at MOI 0.1 for 48 hours to 80% cytopathic effect. Cells were recovered by scraping and frozen/thawed thrice. Titers ranged from 4.2×10^7 to 4.8×10^8 pfu/ml in Vero-E6-USAMRIID plaque assay (85) before inactivation. After UV light (900 mJ/cm^2) and three cycles of freeze-thaw, plaque assays were negative on Vero-E6-USAMRIID. Vero mock antigen was prepared in parallel. Full-length SARS-CoV-2 codon-optimized molecular clones non-structural protein (NSP)1-NSP10, NSP12-NSP16, S, ORF3A, ORF3B, E, M, N, ORF6, ORF7A, ORF7B, ORF8, N, ORF9B, ORF9C (also known as ORF9Bwu and ORF14) from Wuhan-Hu-1 (Wu-1, Genbank NC_045512.2), and ORF10 from strain HKU-SZ-005b (Genbank MN975262.1) cloned into pDONR207 or pDONR223 (29) (ThermoFisher, Waltham, MA), were obtained from Addgene (Waterton, MA). Gateway™ reactions (ThermoFisher) shuttled inserts to expression vectors pDEST103 and pDEST203 for CD8 and CD4 T cell research (30). pDEST103 expresses proteins intracellularly as fusions after N-terminal eGFP driven by a CMV promoter. pDEST203 expresses 6-histidine fusion proteins under the control of a T7 promoter and is used (30) to express antigens via *in vitro* transcription/translation (IVTT)

(Expressway, ThermoFisher). SARS-CoV-2 S Wu-1 with the D614G mutation, HDM_Spikedelta21_D614G (Addgene #158762), and isogenic mutant K417N are described (86, 87). Additional plasmids were designed per S consensus data (22) (88) concordant with representative sequences from GISAID (89) (EPI_ISL_760400 (B.1.1.7 lineage) and EPI_ISL_700420 (B.1.351 lineage)). These were designed with the same 21 aa C-terminal deletion as Wu-1 D614G and D614G/K417N and synthesized and cloned by Twist (South San Francisco, CA) into pHDM to create HDM_Spikedelta21_B.1.351 and HDM_Spikedelta21_B.1.1.7 for transient transfection of eukaryotic cells. The predicted polypeptide sequences of strains WA1 used for PBMC stimulation, Wu-1 used for most peptides differ at ORF8 aa 84 with an S residue in WA1 and L in Wu-1.

sCoV OC43 (NR-52725), 229E (NR-52726), and NL63 (NR-470) were obtained from BEI Resources. OC43 was cultured on VERO E6 AT cells stably transduced with angiotensin converting enzyme 2 (ACE2) and transmembrane serine protease 2 (gift from Michael S. Diamond, Washington University, St. Louis, USA), 229E was cultured on Huh7 cells (90) and NL63 cultured on MK2-LLC cells (CCL-7, ATCC). Antigen was prepared by freeze-thaw and clarification (400 x g, 10 min, room temperature) of infected cells and UV-inactivated, with mock uninfected cell antigens prepared in parallel. Viral titers measured in the producer cells prior to UV were 1.6×10^5 $TCID_{50}$/ml (OC43), 2.3×10^6 $TCID_{50}$/ml (229E) and 2.0×10^2 $TCID_{50}$/ml (NL63). Antigens were tested at 1:40 (v/v) in T cell assays. S genes from OC43, 229E, NL63 and HKU1 (R619-M89-303, R619-M66-303, R619-M90-303, R619-M91-303; 166014, 166015, 166016, 166017, all Addgene) were subcloned into pDEST203 (91). IVTT-expressed antigens were tested at 1:1000.

Peptides covering the SARS-CoV-2 strain Wu-1 predicted proteome, 13 aa long overlapping by 9 aa, were obtained at ≥70% purity (Genscript, Piscataway, NJ) and dissolved at 20 mg/ml in DMSO (ThermoFisher). Peptides in SARS-CoV-2 ORFs polypeptides PP1a and PP1ab are numbered by positions in the polypeptide rather than within non-structural proteins (NSPs). Pools contained ≤ 54 peptides, maintaining 1 μg/ml final in-assay concentrations each, and ≤ 0.3% DMSO. Selected peptides containing variant aa, peptides shorter than 13 aa predicted to bind to HLA class I alleles, or peptides internal to antigenic peptides were also studied. Variants surveyed included variant 501Y.V1 lineage B.1.1.7 (alpha) (92), variant B501Y.V2 lineage B.1.351 (beta) (22), variant 501Y.V3 P.1 lineage, (gamma) (93), and lineage B.1.617.2, (delta) (nomenclature per US CDC Oct 2021 https://www.cdc.gov/coronavirus/2019-ncov/variants/variant-info.html#Interest). sCoV homologs for defined SARS-CoV-2 Wu-1 epitopes in S, N, and M proteins were determined by sequence alignment. If ≥ 1 sCoV homolog, amongst OC43, HKU1, 229E, and NL63, had identity at ≥ 7 aa with antigenic peptides from SARS-CoV-2 Wu-1, 13 aa homologs of the antigenic SARS-CoV-2 peptide from all 4 sCoV were assayed. In addition, OC43 S peptides, 15 aa long/11 aa overlap (EMPS-OC43-S-1, JPT, Berlin, Germany) were tested as pools or single peptides at 1 μg/ml final in ≤ 0.4% DMSO.

SARS-CoV-2-specific T cell enrichment and expansion. For DC-AIM-based enrichment, monocytes were enriched (CD14 positive, Stemcell) and cultured in serum-free AIM-V (Stemcell) with 10 ng/ml each IL-4 and GM-CSF (R&D, Minneapolis, MN) in 6-well plates. Monocyte-origin DC (moDC) were collected at day 7 with EDTA/scraping, and seeded at 2.5 x 10^5/well in 48-well plates. SARS-CoV-2 antigen was loaded into moDC by adding 25 μl UV-killed virus or mock antigen in 1 ml T cell medium (TCM). After 4 hours, 2 x 10^6 autologous total T cells (negative selection, Stemcell) were added for 18 hours. Cells were stained with anti-CD3-PE (BioLegend, UCHT1), anti-CD4-APC-Cy7 (Becton Dickinson, RPA-T4), anti-CD8-FITC (ThermoFisher 3B5), anti-CD69-BV421 or PE-Cy7 (BioLegend, FN50), anti-CD137-APC

(Becton Dickinson, 4B4-1), and 7-actinomycin D (7-AAD). Live $CD3^+CD4^+CD8^-$ or $CD4^-CD8^+$ cells with CD137 and CD69 expression were bulk-sorted and 20% of sorted cells were non-specifically expanded for two cycles (94), with 80% saved for TCR sequencing. moDC were also used to present single viral proteins. HeLa cells (CCL-2, ATCC) were transfected with SARS-CoV-2 genes cloned into pDEST103, or pDEST103 control, using FuGene 6 (Promega) and collected at 48 hours. Transfected cells were suspended to 1 x 10^6 cells/ml and UV-C-treated in a 6-well plate with 3600 μJ/cm^2. moDC were collected at day 7 with EDTA and 1 x 10^5 moDC in 0.4 ml TCM were seeded into 48-well plates for 4 hours prior to adding 1 x 10^5 UV-treated HeLa for one hour. 1.5 x 10^6 autologous PBMC in 0.1 ml were added at 37°C for 18 hours. AIM sorting was also used after stimulation of PBMC without moDC addition. For whole virus, UV-inactivated SARS-CoV-2 was incubated at 1:20 to 1:40 dilution with 1.5 x 10^6 PBMC in 0.2 ml TCM in 96 well U-bottom plates for 18 hours. Mock virus negative control and 1.6 μg/ml phytohemagglutinin (PHA)-P (Remel, Lenexa, KS) positive control were included. For viral proteins, SARS-CoV-2 individual ORFs in pDEST103 were transfected into and expressed by COS-7 cells (#CRL-1651, ATCC, Manassas, VA), which were lysed with three cycles of freeze-thaw treatment. Pooled lysates representing multiple SARS-CoV-2 proteins were added to PBMC at a 1:1 volume ratio for 18 hours.

For proliferation-based enrichment, PBMC were labeled with cell-trace violet (CTV) (ThermoFisher) and cultured at 4 x 10^6/well in 24-well plates in 2 ml (TCM) (25) for 5 days with SARS-CoV-2 peptide pools (≤ 54 peptides/pool, 1 μg/ml final each) covering S (6 pools), M (one pool), N (two pools), or NSP6 and E proteins (2 pools). After staining with anti-CD3-PE, anti-CD4-APC (ThermoFisher, S3.5), anti-CD8-FITC, and 7-AAD for viability, live $CD3^+CTV^{low}$ cells with $CD4^-CD8^+$ or $CD4^+CD8^-$ phenotype were bulk-sorted (FACSARIA II, Becton Dickinson). Polyclonal CTV^{low} T cell lines were expanded twice polyclonally (94).

Tetramer sorting. Monomeric HLA-β2M complexes with UV-labile peptide (BioLegend) were used for UV peptide exchange and tetramerized with streptavidin-APC or streptavidin-PE (Becton Dickinson) per the manufacturer. Bulk-expanded CD8 T cells (~10^6) were stained in 100 µl TCM with 2 µl tetramer for 30 minutes on ice, followed by anti-CD4-APC-H7 and anti-CD8α-FITC. After 7-AAD staining, live $CD8^+CD4^-tetramer^{high}$ cells were sorted, expanded (94), and cryopreserved. CD8 T cells recognizing Merkel cell polyomavirus (MCPyV) T antigen (T-Ag) aa 32-40/HLA A*03:01 were tetramer-sorted from Merkel cell carcinoma tumor-infiltrating lymphocytes (28).

T-cell functional assays. CD8 TCL reactivity to viral proteins was measured using COS-7 artificial antigen presenting cells (aAPC) co-transfected with subject-specific HLA class I cDNA and SARS-CoV-2 ORFs, or fragments of SARS-CoV-2 ORF1a/1ab (95). HLA A and B cDNA alleles were amplified by RT-PCR (94) or synthesized (Genscript), cloned into pcDNA3.1(-) (ThermoFisher) (96) and sequence-verified. COS-7 in 96-well flat plates were co-transfected with 100 ng/well each HLA cDNA and SARS-CoV-2-p103 plasmids, using FuGene6 (96). After 2 days, 1 x 10^5 CD8 TCL/well were added for 24-48 hours into 200 µl TCM, and secreted IFN-gamma (IFN-γ) measured by ELISA (96). For CD8 T cell responses to peptides, aAPC expressed HLA cDNA only. At 2 days, 1-10 µg/ml viral peptide or DMSO control was added with responder TCL, or aAPC were peptide-pulsed for 1 hour at 37 ^oC, 5% CO2 and washed prior to adding TCL. Alternatively, peptide specificity assays used autologous EBV-lymphocyte continuous line (EBV-LCL) as APC at 2-5 x 10^4 cells/well in 96-well U-bottom plates, in duplicate or triplicate, with 5-10 x 10^5 CD8 TCL responders/well. Single or pooled peptides were added at 1 µg/ml each final in ≤ 0.3% DMSO. For a peptide to be listed as a CD8 T cell epitope, we required recognition (IFN-γ OD_{450} > 2X DMSO control) of 1 µg/ml or less peptide in ≥ 2 independent assays. To measure CD8 T cell recognition of SARS-CoV-2-infected cells, human bronchial epithelial cell 3 immortalized with cyclin dependent kinase 4 and human telomerase

599 reverse transcriptase (HBEC3-KT) (97) transduced with ACE2 (44) (HBE3-KT-A) were infected
600 at MOI 2 in 6-well plates using strain WA1-GFP (gift of Dr. Ralph Baric), or mock-infected, for 24
601 hours, harvested with Accutase (Thermo-Fisher) and plated at 20,000 cells/well in 96 well U-
602 bottom plates. CD8 T cells were added (100,000/well) to a final volume of 200 µl TCM.
603 Supernatants after 24 hours were assayed by IFN-γ ELISA (98).
604
605 CD4 T cell assays for whole virus and IVTT proteins used PBMC as APC. In duplicate or
606 triplicate 96-well U-bottoms, 5-10 x 10^4 each autologous PBMC and CD4 TCL were seeded in
607 200 µl TCM, with whole UV-treated SARS-CoV-2 or mock antigen (1:20-1:40), IVTT
608 preparations (1:1000-1:2000) from SARS-CoV-2 or empty vector or HSV-2 gene-containing (99)
609 negative controls, single or pooled peptides or DMSO control, or PHA-P (1.6 µg/ml) positive
610 control. T cell activation was determined by supernatant IFN-γ by ELISA at 1-2 days or ^{3}H
611 thymidine incorporation (proliferation assay at day 3-day 4 (100). When proliferation was
612 measured, autologous PBMC were irradiated (3,300 rad, X-ray source). The criteria for positivity
613 were that in duplicate assays, both raw CPM values were at least twice the average of the
614 negative control wells containing irrelevant HSV antigens and media.
615
616 Alternatively, responses to whole virus and IVTT proteins were measured by intracellular
617 cytokine secretion (ICS). Polyclonal CD4 TCL were CTV-labeled (25). Autologous PBMC and
618 CD4 TCL (2-5 x 10^5 each) were co-incubated in 200 µl TCM in 96-well U-bottoms with antigens
619 or controls at concentrations listed above. Co-stimulatory mAbs (anti-CD28 and anti-CD49d,
620 BioLegend) and Brefeldin A were added (25) and cells analyzed after 16-18 hours. Cells were
621 stained with Near-IR live/dead (ThermoFisher), lysed with 1X FACS lysing solution (Becton
622 Dickinson), permeabilization with FACS Perm 2 (Becton Dickinson), and stained with anti-CD3-
623 PE, anti-CD4-FITC (ThermoFisher, S3.5), and anti-CD8-PerCP5.5 (SK1), anti-IFN-γ-PE-Cy7,
624 (B27, Becton Dickson) and anti-IL-2 (MQ1-17H12, Becton Dickinson). Data were acquired with

FACSCANTO and cytokine expression quantified for live, CTV-positive $CD3^+CD4^+CD8^-$ single cells (FlowJo 10.7.1, Becton Dickinson). For ICS-based proteome screens of CD4 TCL, two criteria were both required to score a protein positive. The ratio of the percent of IFN-γ and/or IL-2 positive CD4 T cells with SARS-CoV-2 antigen compared with pDEST203 empty vector-derived IVTT product, was > 2. For subjects W002 and W011 with high IFN-γ background for pDEST203 empty vector, the percent of double-positive IFN-γ/IL-2 cells, only, was used. Second, the difference in cytokine-positive cells between a SARS-CoV-2 protein and empty vector was > 1%.

CD4 T cell peptide analyses used autologous EBV-LCL as APC. TCL (2-5 x 10^4/well) and EBV-LCL (5-20 X 10^3/well) were co-plated in 96-well U plates in duplicate or triplicate in 200 µl TCM. Peptides at 1 µg/ml each final concentration were added as pools or singletons in ≤0.3% DMSO, or DMSO negative control. After 1 to 2 days, supernatant IFN-γ was measured by ELISA. For some assays with high IFN-γ ELISA OD_{450} values for negative control stimuli, ELISA was performed with diluted supernatants. In order for a peptide to be reported as an epitope, two or more wells tested with 1 µg/ml peptide were required to have an IFN-γ OD_{450} at least twice above DMSO background in at least two assays. For proliferation assays, peptides (1 µg/ml) were tested using autologous EBV-LCL (1 X 10^4/well, irradiated 10,000 rad) and responder TCL (5 X 10^4/well) in duplicate. For a peptide to be reported as an epitope, both replicates had a count per minute (CPM) value more than 2-fold the average CPM of DMSO negative controls, and, in follow-up triplicate screens, at least two of the three CPM values were more than 2-fold average CPM of negative controls. To enumerate CD4 T cell reactivities per-subject, each reactive peptide was counted as a separate epitope. If two variant SARS-CoV-2 peptides were reactive for the same person, this was counted as one reactivity. Reactivities detected in more than one workflow or PBMC timepoint per person are counted once.

Responses to the same or variant peptides in multiple participants were analyzed both separately and after collapse to unique peptides.

We defined CD4 TCL HLA restriction as published (40). First, serial dilutions of peptide (1, 0.1, or 0.01 µg/ml) were tested in triplicate using autologous EBV-LCL as APC without or with mAbs that block HLA DR, DP, or DQ (100). To determine allele-level restriction, engineered APC expressing single HLA class II heterodimers were selected (40) to match the study subject. Negative controls were cells parental to the single antigen line (SAL). SAL assays typically used 1 µg/ml peptide or DMSO control. Some used SAL washed after a 1-hour pulse at 37 ^{o}C with peptides in titration. CD4 TCL were added and IFN-γ secretion measured by ELISA. To estimate functional avidit, we set an index value of 100% to the difference between the mean IFN-γ OD_{450} values of 1 µg/ml peptide and of DMSO. A peptide concentration was scored as positive if at least two of three triplicates at that concentration yielded net IFN-γ OD_{450} values (raw values minus the mean of DMSO) at least 30% of this index value. For selected peptide epitopes an alternative or expanded dilution series was used.

TCR sequencing and analysis. AIM (+) PBMC were flash frozen after sorting in a minimal volume of TCM and DNA manually isolated with the Qiagen blood kit for small samples. DNA from culture-expanded AIM (+) cells was isolated by Adaptive. T cell receptor beta (*TRB)* complementarity determining region 3 (CDR3) repertoire sequencing was performed at Adaptive Biotechnologies (Seattle, WA) using the Immunoseq^{TM} TCRBv4b platform. Two replicate DNA aliquots were processed in parallel and only productive TRB CDR3 gene rearrangements present in at least one read in both replicates were reported. Analyses focused on functional CDR3 amino acid identity.

675 **Data availability.** T cell epitopes have been uploaded to IEDB(102) with accession numbers
676 1000861 and 1000866. TCR datasets are in ImmuneACCESS (Adaptive).
677
678 **Approval.** By the University of Washington Institutional Review Board as Study00004312.
679
680 **Statistics and variant abundance.** Proportions of *ex vivo* AIM (+) cells were compared within-
681 person between mock and stimulated conditions using Wilcoxon matched-pairs signed-ranks
682 test (Instat 3.10, GraphPad, San Diego, CA). Proportions of *ex vivo* AIM (+) cells after
683 stimulation were compared between clinical cohorts using Mann-Whitney test. P values are two-
684 tailed. Correlation between IFN-γ and proliferation results used linear regression and default
685 parameters (Prism 9.1.0, GraphPad). To estimate the global prevalence of SARS-CoV-2 amino
686 acid variants, the worldwide SARS-CoV-2 sequence dataset hosted at GISAID (89) was
687 accessed (101) using the mutation details routine, while lineages containing specific mutations
688 were queried via Nextstrain (23), which accesses a representative subset of GISAID.
689

690

691 Table 1. Summary of varied T cell recognition of SARS-CoV-2 peptides from strain Wu-1 and variants.

T cell phenotype	HLA restriction [1]	protein	peptide [2]	Wu-1 [3]	variant	variant recognition [4]	predicted HLA binding effect [5]	PANGO lineage(s) [6]	prevalence [7]
CD4	DR	S	37-49	YYPDKVFRSSVLH	H49Y	reduced	not applicable	B.1, others	0.19%
CD4	DRB1*07:01, DRB1*15:01	S	61-73	NVTWFHAIHVSGT	del69-70	not detected	moderate decrement *07:01; large decrement *15:01	B.1.1.7	23.76%
CD4	DRB1*11:01	S	61-73	NVTWFHAIHVSGT	del69-70	not detected	large decrement	B.1.1.7	23.76%
CD4	DP, likely A1*01:03/B1*04:01	S	133-145	FQFCN**D**PFLGVYY	D138Y	reduced	no effect	B.1.351	2.46%
CD4	DP, likely A1*01:03/B1*04:01	S	133-145	FQFCNDPFL**G**VYY	G142D	reduced	no effect	B.1.617.2	28.77%
CD4	DP, likely A1*01:03/B1*04:01	S	133-145	FQFCNDPFLGV**Y**Y	Y144del	reduced	moderate decrement	B.1.1.7	23.46%
CD4	DP, likely A1*01:03/B1*04:01	S	165-177	NCTFEYVSQPFLM	L176F	reduced, not detected	no effect	multiple	0.19%
CD4	DR	S	165-177	NCTFEYVSQPFLM	L176F	reduced	not applicable	multiple	0.19%
CD4	DR [8]	S	209-221	PINLVRDLPQGFS	D215H	not detected	no effect	multiple	0.08%
CD4	DR [8]	S	209-221	PINLVRDLPQGFS	D215G	not detected	moderate/large decrement	B.1.351	0.78%
CD4	DR	S	233-245	INITRFQT**LLA**LH	del242-244	not detected	no effect/moderate decrement	B.1.351	0.75%
CD8	A*02:01	S	269-277	YLQPRTFLL	P272L	not detected	no effect	B.1.177	0.23%
CD8	A*03:01	S	378-386	KCYGVSPTK	K378N	not detected	moderate decrement	n/a	0.01%
CD8	A*02:01	S	417-425	KIADYNYKL	K417N	not detected	no effect	B.1.351	0.93%
CD8	A*02:01	S	417-425	KIADYNYKL	K417T	not detected	no effect	P.1	2.26%
CD4	DR	S	485-497	GFNCYFPLQSYGF	F490S	not detected	not applicable	multiple	0.29%
CD8	A*29:02	S	489-497	YFPLQSYGF	F490S	not detected	moderate decrement	multiple	0.29%
CD4	unknown	S	665-677	PIGAGICASYQTQ	Q677H	increased	not applicable	multiple	1.10%
CD4	unknown	S	693-705	IAYTMSLG**A**ENSV	A701V	reduced	no effect	B.1.351	1.59%
CD4	DRB1*07:01; DRB1*04:07/DRB4*01:03 [9]	S	717-729	NFTISVTTEILPV	T723I	reduced	moderate decrement	B.1.389	0.03%
CD4	DR	S	973-985	ISSVLNDILSRLD	S982A	not detected	not applicable	B.1.1.7	23.81%

CD4	DR	S	1017-1029	EIRASANLAA**T**KM	T1027I	reduced	no effect	P.1	2.53%
CD4	DRB1*03:01	S	1113-1125	QIITTDNTFVSGN	D1118H	not detected	large decrement	B.1.1.7	23.81%
CD4	DQ	N	13-25	PRITFGGPSDSTG	P13L	reduced	not applicable	B.6.8, B.1.1.1, others	0.69%
CD4	DR	N	217-229	AALALLLLDRLNQ	A220V	neutral	not applicable	B.1.177.72, others	3.62%
CD4	unknown	N	201-213	SSRGTSPARMAGN	203/204	not detected		multiple	30.07%
CD4	unknown	NSP6	3601-3613	SLFFFLYENAFLP	L3606F	not detected	not applicable	B.6.8, many others	2.48%
CD4	unknown	ORF3A	241-253	EEHVQIHTIDGSS	G251V	not detected	not applicable	multiple	0.16%
CD8	A*11:01	M	169-181	TVATSRTLSYYKL	T175M	not detected	no effect	B.1.1	0.05%

[1] Restricting locus for CD8 T cells proven using aAPC, and available information for CD4 T cells using locus-blocking mAbs and/or SAL.

[2] Amino acid number in protein in SARS-CoV-2 strain Wu-1 proteome. For NSP6, position in ORF1ab polypeptide.

[3] Amino acid sequence in SARS-CpoV-2 strain Wu-1.

[4] Summary of experimental data in this report. If differing effects are seen for > 1 participants' T cells, both results are listed. Not detected signifies >90% reduction in mean net IFN-γ OD_{450} at 1 μg/ml peptide.

[5] Summary of predicted HLA binding to implicated HLA restricting allele, if determined, from consensus algorithms at http://tools.iedb.org/main/tcell/

[6] Derived from representative sampling of ~ 3500 worldwide complete sequences at https://nextstrain.org/ accessed Nov 2021. Lineages include B.1.1.7, also known as alpha, B.1.351, also known as beta, B.1.617.2, also known as delta, P.1, also known as gamma.

705 [7] Worldwide cumulative prevalence at https://covid19dashboard.regeneron.com/?tab=Mutation_Details accessed Nov 2021.

706 [8] DRB1*03:01 in one subject, DR locus in 2nd subject.

707 [9] Responses in one subject DRB1*07:01 restricted; in 2nd subject restricted by both alleles shown; significantly reduced recognition

708 of variant for both subjects using autologous EBV-LCL as APC.

Figure legends

Fig. 1. AIM detection and enrichment of SARS-CoV-2 specific T cells in response to whole virus. A: PBMC from participant W003 incubated with inactivated cell-associated SARS-CoV-2 or mock antigen. Gating scheme at top. Lower panels show expression of activation markers CD137 and CD69 in response to 18 hour stimulation amongst CD4 or CD8 T cells. B: Similar layout for subject W005, specimen 1 PBMC stimulated with autologous moDC pre-treated with SARS-CoV-2 or mock antigen. Gating scheme at top. For both stimulation methods, numbers are percentages of gated T cells expressing dual activation markers. C: CD69/CD137 positive CD4 T cells from the pathway in part A: were expanded and tested for reactivity with inactivated cell-associated SARS-CoV-2 or mock antigen. Gated, live, responder, CD3+/CD4+/CD8-cells are shown. Numbers are percent of cells accumulating the indicated cytokines.

Fig. 2. Recognition of infected respiratory epithelial cells by SARS-CoV-2-specific CD8 T cells. A: HBEC3-KT-A cells with or without infection with SARS-CoV-2 were co-cultivated with tetramer-enriched, HLA A*03:01-restricted, S 378-386-specific CD8 T cells and activation measured by IFN-γ secretion. S: S-specific T cells. M: control MCPyV-specific CD8 T cells. B: Both T cell populations specifically recognized HBEC3-KT-A cells treated with relevant viral peptide.

Fig. 3. SARS-CoV-2 CD8 T cell antigens and epitopes from PBMC stimulation with whole SARS-CoV-2 antigen. A: Subject W005, specimen 1 CD8 TCL were assayed with aAPC expressing each SARS-CoV-2 protein and relevant HLA A and B. Four reactivities were noted. B: Subject W010 CD8 TCL is reactive with HLA A*01:01 aAPC co-transfected with NSP3. For A: and B: negative controls at right. C: CD8 TCL from B: assayed against column (C) and row (R) pooled NSP3 peptides with autologous EBV-LCL as APC. D: Tetramer stain of CD8 TCL before

and after sorting and expansion of tetramer-positive cells. Percentages of tetramer-positive cells shown E: Reactivity of tetramer-enriched cells for aAPC transfected with the indicated plasmids or treated with the indicated peptides. F: Dose-response for HLA A*01:01 aAPC with the indicated concentrations of NSP3 1637-1646. Duplicate or triplicate IFN-γ release assays show raw data as bars (A) or dots for each value and means as bars (B, C, E, F).

Fig. 4. Summary of SARS-CoV-2 proteome-level T cell reactivity for PBMC after COVID-19 illness, using AIM enrichment with whole viral antigen. Rows indicate donors and days between recovery from illness and PBMC sampling. Upper 5 rows were studied without DC boosting; lower 12 rows used this procedure. Columns are individual SARS-CoV-2 proteins. A: CD8 TCL scoring positive (purple). B: CD4 TCL scoring positive (red). At right are number of proteins recognized and at bottom are number of subjects with reactivity at one or more time points.

Fig. 5. A: CD4 TCL from PBMC stimulated with moDC and whole SARS-CoV-2 (subjects W001, W005, W012) or PBMC stimulated with whole SARS-CoV-2 (subject W003) recognize whole SARS-CoV-2, and sCoVOC43 or 229E antigens (V), but not mock (M) antigens. B: CD4 TCL from subject W001 recognizes full-length S protein from OC43 but not empty vector control. C: CD4 TCL recognize homologous S peptides from SARS-CoV-2 and OC43 in an HLA DR-restricted fashion as indicated by inhibition with locus-specific mAb. An overlapping SARS-CoV-2 peptide shows DRB1*15:01 restriction at right. Conserved AA are underlined.

Fig. 6. CD8 TCL recognition by SARS-CoV-2 variant peptides. aAPC transfected with HLA A*02:01 and treated with wild-type but not variant peptides were recognized by polyclonal CD8 TCL lines. Lineage B.1.351 is also known as beta and P.1 is also known as gamma).

Fig. 7. CD4 TCL recognition by SARS-CoV-2 variant peptides. Summary of recognition of S strain Wu-1 peptides and variants. Donors indicated at top. Each Wu-1 peptide recognized by one or more subject is numbered at left. Coordinates and AA substitutions or deletions of variants tested are listed at right. Variants in WHO VOC indicated with blue square. Color codes at left summarize level of recognition of variant peptide by each TCL. VBM = variants being monitored, VOC = variants of concern per US CDC October 2021.

766

References

1. Hansen CH, Michlmayr D, Gubbels SM, Mølbak K, and Ethelberg S. Assessment of protection against reinfection with SARS-CoV-2 among 4 million PCR-tested individuals in Denmark in 2020: a population-level observational study. *Lancet (London, England).* 2021.
2. Topol EJ. Messenger RNA vaccines against SARS-CoV-2. *Cell.* 2021;184(6):1401.
3. McMahan K, Yu J, Mercado NB, Loos C, Tostanoski LH, Chandrashekar A, et al. Correlates of protection against SARS-CoV-2 in rhesus macaques. *Nature.* 2021;590(7847):630-4.
4. Tarke A, Sidney J, Kidd CK, Dan JM, Ramirez SI, Yu ED, et al. Comprehensive analysis of T cell immunodominance and immunoprevalence of SARS-CoV-2 epitopes in COVID-19 cases. *Cell reports Medicine.* 2021;2(2):100204.
5. Snyder TM, Gittelman RM, Klinger M, May DH, Osborne EJ, Taniguchi R, et al. Magnitude and Dynamics of the T-Cell Response to SARS-CoV-2 Infection at Both Individual and Population Levels. *medRxiv.* 2020.
6. Braun J, Loyal L, Frentsch M, Wendisch D, Georg P, Kurth F, et al. SARS-CoV-2-reactive T cells in healthy donors and patients with COVID-19. *Nature.* 2020;587(7833):270-4.
7. Boonyaratanakornkit J, Morishima C, Selke S, Zamora D, McGuffin S, Shapiro AE, et al. Clinical, laboratory, and temporal predictors of neutralizing antibodies against SARS-CoV-2 among COVID-19 convalescent plasma donor candidates. *The Journal of clinical investigation.* 2021;131(3).
8. Yu KK, Fischinger S, Smith MT, Atyeo C, Cizmeci D, Wolf CR, et al. Comorbid illnesses are associated with altered adaptive immune responses to SARS-CoV-2. *JCI Insight.* 2021.
9. Elyanow R, Snyder TM, Dalai SC, Gittelman RM, Boonyaratanakornkit J, Wald A, et al. T-cell receptor sequencing identifies prior SARS-CoV-2 infection and correlates with neutralizing antibody titers and disease severity. *medRxiv : the preprint server for health sciences.* 2021:2021.03.19.21251426. In Revision, Journal of Clinical Investigation.
10. Phan IQ, Subramanian S, Kim D, Murphy M, Pettie D, Carter L, et al. In silico detection of SARS-CoV-2 specific B-cell epitopes and validation in ELISA for serological diagnosis of COVID-19. *Scientific reports.* 2021;11(1):4290.
11. Grifoni A, Weiskopf D, Ramirez SI, Mateus J, Dan JM, Moderbacher CR, et al. Targets of T Cell Responses to SARS-CoV-2 Coronavirus in Humans with COVID-19 Disease and Unexposed Individuals. *Cell.* 2020;181(7):1489-501.e15.
12. Dan JM, Mateus J, Kato Y, Hastie KM, Yu ED, Faliti CE, et al. Immunological memory to SARS-CoV-2 assessed for up to eight months after infection. *bioRxiv : the preprint server for biology.* 2020.
13. Clute SC, Naumov YN, Watkin LB, Aslan N, Sullivan JL, Thorley-Lawson DA, et al. Broad cross-reactive TCR repertoires recognizing dissimilar Epstein-Barr and influenza A virus epitopes. *J Immunol.* 2010;185(11):6753-64.
14. Vuorela A, Freitag TL, Leskinen K, Pessa H, Härkönen T, Stracenski I, et al. Enhanced influenza A H1N1 T cell epitope recognition and cross-reactivity to protein-O-mannosyltransferase 1 in Pandemrix-associated narcolepsy type 1. *Nature communications.* 2021;12(1):2283.
15. Chiou SH, Tseng D, Reuben A, Mallajosyula V, Molina IS, Conley S, et al. Global analysis of shared T cell specificities in human non-small cell lung cancer enables HLA inference and antigen discovery. *Immunity.* 2021;54(3):586-602.e8.
16. Huisman W, Leboux DAT, van der Maarel LE, Hageman L, Amsen D, Falkenburg JHF, et al. Magnitude of Off-Target Allo-HLA Reactivity by Third-Party Donor-Derived Virus-Specific T Cells Is Dictated by HLA-Restriction. *Frontiers in immunology.* 2021;12:630440.

17. Koelle DM, Chen HB, McClurkan CM, and Petersdorf EW. Herpes simplex virus type 2-specific CD8 cytotoxic T lymphocyte cross-reactivity against prevalent HLA class I alleles. *Blood.* 2002;99(10):3844-7.
18. Hammer GE, Kanaseki T, and Shastri N. The final touches make perfect the peptide-MHC class I repertoire. *Immunity.* 2007;26(4):397-406.
19. Starck SR, and Shastri N. Nowhere to hide: unconventional translation yields cryptic peptides for immune surveillance. *Immunological reviews.* 2016;272(1):8-16.
20. Lineburg KE, Grant EJ, Swaminathan S, Chatzileontiadou DSM, Szeto C, Sloane H, et al. CD8(+) T cells specific for an immunodominant SARS-CoV-2 nucleocapsid epitope cross-react with selective seasonal coronaviruses. *Immunity.* 2021;54(5):1055-65.e5.
21. McCarthy KR, Rennick LJ, Nambulli S, Robinson-McCarthy LR, Bain WG, Haidar G, et al. Recurrent deletions in the SARS-CoV-2 spike glycoprotein drive antibody escape. *Science (New York, NY).* 2021;371(6534):1139-42.
22. Tegally H, Wilkinson E, Giovanetti M, Iranzadeh A, Fonseca V, Giandhari J, et al. Emergence of a SARS-CoV-2 variant of concern with mutations in spike glycoprotein. *Nature.* 2021.
23. Hadfield J, Megill C, Bell SM, Huddleston J, Potter B, Callender C, et al. Nextstrain: real-time tracking of pathogen evolution. *Bioinformatics (Oxford, England).* 2018;34(23):4121-3.
24. Bouhaddou M, Memon D, Meyer B, White KM, Rezelj VV, Correa Marrero M, et al. The Global Phosphorylation Landscape of SARS-CoV-2 Infection. *Cell.* 2020;182(3):685-712.e19.
25. Hanson DJ, Tsvetkova O, Rerolle GF, Greninger AL, Sette A, Jing L, et al. Genome-Wide Approach to the CD4 T-Cell Response to Human Herpesvirus 6B. *J Virol.* 2019;93(14).
26. DeWitt WS, Emerson RO, Lindau P, Vignali M, Snyder TM, Desmarais C, et al. Dynamics of the cytotoxic T cell response to a model of acute viral infection. *J Virol.* 2015;89(8):4517-26.
27. Ferretti AP, Kula T, Wang Y, Nguyen DMV, Weinheimer A, Dunlap GS, et al. Unbiased Screens Show CD8(+) T Cells of COVID-19 Patients Recognize Shared Epitopes in SARS-CoV-2 that Largely Reside outside the Spike Protein. *Immunity.* 2020;53(5):1095-107.e3.
28. Jing L, Ott M, Church CD, Kulikauskas RM, Ibrani D, Iyer JG, et al. Prevalent and Diverse Intratumoral Oncoprotein-Specific CD8(+) T Cells within Polyomavirus-Driven Merkel Cell Carcinomas. *Cancer immunology research.* 2020;8(5):648-59.
29. Kim DK, Knapp JJ, Kuang D, Chawla A, Cassonnet P, Lee H, et al. A Comprehensive, Flexible Collection of SARS-CoV-2 Coding Regions. *G3 (Bethesda, Md).* 2020;10(9):3399-402.
30. Jing L, Haas, J., Chong, T.M., Bruckner, J.J., Dann, G.C., Dong, L., Marshak, J.O., McClurkan, C.L., Yamamoto, T.N., Bailer, S.M., Laing, K.J., Wald, A., Verjans, G.M.G.M., Koelle, D.M. Herpes simplex virus type 1 T-cells antigens in humans revealed by cross-presentation and genome-wide screening. *Journal of Clinical Investigation.* 2012;122:654-73.
31. Sette A, and Crotty S. Adaptive immunity to SARS-CoV-2 and COVID-19. *Cell.* 2021;184(4):861-80.
32. Le Bert N, Clapham HE, Tan AT, Chia WN, Tham CYL, Lim JM, et al. Highly functional virus-specific cellular immune response in asymptomatic SARS-CoV-2 infection. *J Exp Med.* 2021;218(5).
33. Wyllie D, Jones HE, Mulchandani R, Trickey A, Taylor-Phillips S, Brooks T, et al. SARS-CoV-2 responsive T cell numbers and anti-Spike IgG levels are both associated with protection from COVID-19: A prospective cohort study in keyworkers. *medRxiv.* 2021:2020.11.02.20222778.
34. Van Damme KFA, Tavernier S, Van Roy N, De Leeuw E, Declercq J, Bosteels C, et al. Case Report: Convalescent Plasma, a Targeted Therapy for Patients with CVID and Severe COVID-19. *Frontiers in immunology.* 2020;11:596761.
35. Tarhini H, Recoing A, Bridier-Nahmias A, Rahi M, Lambert C, Martres P, et al. Long term SARS-CoV-2 infectiousness among three immunocompromised patients: from prolonged viral shedding to SARS-CoV-2 superinfection. *The Journal of infectious diseases.* 2021.

36. Shaan Lakshmanappa Y, Elizaldi SR, Roh JW, Schmidt BA, Carroll TD, Weaver KD, et al. SARS-CoV-2 induces robust germinal center CD4 T follicular helper cell responses in rhesus macaques. *Nature communications.* 2021;12(1):541.
37. Blum JS, Wearsch PA, and Cresswell P. Pathways of antigen processing. *Annual review of immunology.* 2013;31:443-73.
38. Matyushenko V, Isakova-Sivak I, Kudryavtsev I, Goshina A, Chistyakova A, Stepanova E, et al. Detection of IFNgamma-Secreting CD4(+) and CD8(+) Memory T Cells in COVID-19 Convalescents after Stimulation of Peripheral Blood Mononuclear Cells with Live SARS-CoV-2. *Viruses.* 2021;13(8).
39. Jing L, Schiffer JT, Chong TM, Bruckner JJ, Davies DH, Felgner PL, et al. CD4 T-cell memory responses to viral infections of humans show pronounced immunodominance independent of duration or viral persistence. *J Virol.* 2013;87(5):2617-27.
40. Campbell VL, Nguyen L, Snoey E, McClurkan CL, Laing KJ, Dong L, et al. Proteome-Wide Zika Virus CD4 T Cell Epitope and HLA Restriction Determination. *Immunohorizons.* 2020;4(8):444-53.
41. Nayak K, Jing L, Russell RM, Davies DH, Hermanson G, Molina DM, et al. Identification of novel Mycobacterium tuberculosis CD4 T-cell antigens via high throughput proteome screening. *Tuberculosis (Edinb).* 2015;95(3):275-87.
42. Laing KJ, Russell RM, Dong L, Schmid DS, Stern M, Magaret A, et al. Zoster vaccination increases the breadth of CD4+ T cells responsive to varicella zoster virus. *The Journal of infectious diseases.* 2015.
43. Diao B, Wang C, Wang R, Feng Z, Zhang J, Yang H, et al. Human kidney is a target for novel severe acute respiratory syndrome coronavirus 2 infection. *Nature communications.* 2021;12(1):2506.
44. Addetia A, Lieberman NAP, Phung Q, Hsiang TY, Xie H, Roychoudhury P, et al. SARS-CoV-2 ORF6 Disrupts Bidirectional Nucleocytoplasmic Transport through Interactions with Rae1 and Nup98. *mBio.* 2021;12(2).
45. Akilesh S, Nicosia RF, Alpers CE, Tretiakova M, Hsiang TY, Gale M, Jr., et al. Characterizing Viral Infection by Electron Microscopy: Lessons from the Coronavirus Disease 2019 Pandemic. *The American journal of pathology.* 2021;191(2):222-7.
46. Lodes N, Seidensticker K, Perniss A, Nietzer S, Oberwinkler H, May T, et al. Investigation on Ciliary Functionality of Different Airway Epithelial Cell Lines in Three-Dimensional Cell Culture. *Tissue engineering Part A.* 2020;26(7-8):432-40.
47. Ahn JH, Kim J, Hong SP, Choi SY, Yang MJ, Ju YS, et al. Nasal ciliated cells are primary targets for SARS-CoV-2 replication in the early stage of COVID-19. *The Journal of clinical investigation.* 2021;131(13).
48. Zhang Y, Chen Y, Li Y, Huang F, Luo B, Yuan Y, et al. The ORF8 protein of SARS-CoV-2 mediates immune evasion through down-regulating MHC-I. *Proceedings of the National Academy of Sciences of the United States of America.* 2021;118(23).
49. Wagner KIea. Recruitment of highly functional SARS-CoV-2-specific CD8+ T cell receptors mediating cytotoxicity of virus-infected target cells in non-severe COVID-19. 2021.
50. Koelle DM, Tigges MA, Burke RL, Symington FW, Riddell SR, Abbo H, et al. Herpes simplex virus infection of human fibroblasts and keratinocytes inhibits recognition by cloned CD8+ cytotoxic T lymphocytes. *Journal of Clinical Investigation.* 1993;91:961-8.
51. Kaneko N, Boucau J, Kuo HH, Perugino C, Mahajan VS, Farmer JR, et al. Expansion of Cytotoxic CD4+ T cells in the lungs in severe COVID-19. *medRxiv.* 2021.
52. Meckiff BJ, Ramirez-Suastegui C, Fajardo V, Chee SJ, Kusnadi A, Simon H, et al. Imbalance of Regulatory and Cytotoxic SARS-CoV-2-Reactive CD4(+) T Cells in COVID-19. *Cell.* 2020;183(5):1340-53 e16.

53. Ramos da Silva S, Ju E, Meng W, Paniz Mondolfi AE, Dacic S, Green A, et al. Broad Severe Acute Respiratory Syndrome Coronavirus 2 Cell Tropism and Immunopathology in Lung Tissues From Fatal Coronavirus Disease 2019. *The Journal of infectious diseases.* 2021;223(11):1842-54.
54. Bojkova D, Klann K, Koch B, Widera M, Krause D, Ciesek S, et al. Proteomics of SARS-CoV-2-infected host cells reveals therapy targets. *Nature.* 2020;583(7816):469-72.
55. Davidson AD, Williamson MK, Lewis S, Shoemark D, Carroll MW, Heesom KJ, et al. Characterisation of the transcriptome and proteome of SARS-CoV-2 reveals a cell passage induced in-frame deletion of the furin-like cleavage site from the spike glycoprotein. *Genome medicine.* 2020;12(1):68.
56. Ihling C, Tänzler D, Hagemann S, Kehlen A, Hüttelmaier S, Arlt C, et al. Mass Spectrometric Identification of SARS-CoV-2 Proteins from Gargle Solution Samples of COVID-19 Patients. *Journal of proteome research.* 2020;19(11):4389-92.
57. Nikolaev EN, Indeykina MI, Brzhozovskiy AG, Bugrova AE, Kononikhin AS, Starodubtseva NL, et al. Mass-Spectrometric Detection of SARS-CoV-2 Virus in Scrapings of the Epithelium of the Nasopharynx of Infected Patients via Nucleocapsid N Protein. *Journal of proteome research.* 2020;19(11):4393-7.
58. Jing L, Chong TM, Byrd B, McClurkan CL, Huang J, Story BT, et al. Dominance and diversity in the primary human CD4 T cell response to replication-competent vaccinia virus. *J Immunol.* 2007;178(10):6374-86.
59. Le Bert N, Tan AT, Kunasegaran K, Tham CYL, Hafezi M, Chia A, et al. SARS-CoV-2-specific T cell immunity in cases of COVID-19 and SARS, and uninfected controls. *Nature.* 2020;584(7821):457-62.
60. Nelde A, Bilich T, Heitmann JS, Maringer Y, Salih HR, Roerden M, et al. SARS-CoV-2-derived peptides define heterologous and COVID-19-induced T cell recognition. *Nature immunology.* 2021;22(1):74-85.
61. Oja AE, Saris A, Ghandour CA, Kragten NAM, Hogema BM, Nossent EJ, et al. Divergent SARS-CoV-2-specific T- and B-cell responses in severe but not mild COVID-19 patients. *European journal of immunology.* 2020;50(12):1998-2012.
62. Peng Y, Mentzer AJ, Liu G, Yao X, Yin Z, Dong D, et al. Broad and strong memory CD4(+) and CD8(+) T cells induced by SARS-CoV-2 in UK convalescent individuals following COVID-19. *Nature immunology.* 2020;21(11):1336-45.
63. Gordon DE, Hiatt J, Bouhaddou M, Rezelj VV, Ulferts S, Braberg H, et al. Comparative host-coronavirus protein interaction networks reveal pan-viral disease mechanisms. *Science (New York, NY).* 2020;370(6521).
64. Jiang HW, Li Y, Zhang HN, Wang W, Yang X, Qi H, et al. SARS-CoV-2 proteome microarray for global profiling of COVID-19 specific IgG and IgM responses. *Nature communications.* 2020;11(1):3581.
65. Wu J, Shi Y, Pan X, Wu S, Hou R, Zhang Y, et al. SARS-CoV-2 ORF9b inhibits RIG-I-MAVS antiviral signaling by interrupting K63-linked ubiquitination of NEMO. *Cell reports.* 2021;34(7):108761.
66. Tarke A, Sidney J, Methot N, Zhang Y, Dan JM, Goodwin B, et al. Negligible impact of SARS-CoV-2 variants on CD4 (+) and CD8 (+) T cell reactivity in COVID-19 exposed donors and vaccinees. *bioRxiv : the preprint server for biology.* 2021.
67. Agerer B, Koblischke M, Gudipati V, Montaño-Gutierrez LF, Smyth M, Popa A, et al. SARS-CoV-2 mutations in MHC-I-restricted epitopes evade CD8(+) T cell responses. *Science immunology.* 2021;6(57).
68. Yang X, Gao M, Chen G, Pierce BG, Lu J, Weng NP, et al. Structural Basis for Clonal Diversity of the Public T Cell Response to a Dominant Human Cytomegalovirus Epitope. *The Journal of biological chemistry.* 2015;290(48):29106-19.

69. Laing KJ, Dong L, Sidney J, Sette A, and Koelle DM. Immunology in the Clinic Review Series; focus on host responses: T cell responses to herpes simplex viruses. *Clin Exp Immunol.* 2012;167(1):47-58.
70. Jing L, Laing KJ, Dong L, Russell RM, Barlow RS, Haas JG, et al. Extensive CD4 and CD8 T Cell Cross-Reactivity between Alphaherpesviruses. *J Immunol.* 2016;196(5):2205-18.
71. de Silva TI, Liu G, Lindsey BB, Dong D, Moore SC, Hsu NS, et al. The impact of viral mutations on recognition by SARS-CoV-2 specific T-cells. *iScience.* 2021:103353.
72. Keeton R, Richardson SI, Moyo-Gwete T, Hermanus T, Tincho MB, Benede N, et al. Prior infection with SARS-CoV-2 boosts and broadens Ad26.COV2.S immunogenicity in a variant-dependent manner. *Cell host & microbe.* 2021.
73. Choi A, Koch M, Wu K, Chu L, Ma L, Hill A, et al. Safety and immunogenicity of SARS-CoV-2 variant mRNA vaccine boosters in healthy adults: an interim analysis. *Nature medicine.* 2021.
74. Mateus J, Grifoni A, Tarke A, Sidney J, Ramirez SI, Dan JM, et al. Selective and cross-reactive SARS-CoV-2 T cell epitopes in unexposed humans. *Science (New York, NY).* 2020;370(6512):89-94.
75. Schmidt KG, Nganou-Makamdop K, Tenbusch M, El Kenz B, Maier C, Lapuente D, et al. SARS-CoV-2-Seronegative Subjects Target CTL Epitopes in the SARS-CoV-2 Nucleoprotein Cross-Reactive to Common Cold Coronaviruses. *Frontiers in immunology.* 2021;12:627568.
76. Mateus J, Dan JM, Zhang Z, Rydyznski Moderbacher C, Lammers M, Goodwin B, et al. Low-dose mRNA-1273 COVID-19 vaccine generates durable memory enhanced by cross-reactive T cells. *Science (New York, NY).* 2021;374(6566):eabj9853.
77. Ng KW, Faulkner N, Wrobel AG, Gamblin SJ, and Kassiotis G. Heterologous humoral immunity to human and zoonotic coronaviruses: Aiming for the achilles heel. *Seminars in immunology.* 2021:101507.
78. Aguilar-Bretones M, Westerhuis BM, Raadsen MP, de Bruin E, Chandler FD, Okba NM, et al. Seasonal coronavirus-specific B cells with limited SARS-CoV-2 cross-reactivity dominate the IgG response in severe COVID-19. *The Journal of clinical investigation.* 2021;131(21).
79. Sagar M, Reifler K, Rossi M, Miller NS, Sinha P, White LF, et al. Recent endemic coronavirus infection is associated with less-severe COVID-19. *The Journal of clinical investigation.* 2021;131(1).
80. Nguyen THO, Rowntree LC, Petersen J, Chua BY, Hensen L, Kedzierski L, et al. CD8(+) T cells specific for an immunodominant SARS-CoV-2 nucleocapsid epitope display high naive precursor frequency and TCR promiscuity. *Immunity.* 2021;54(5):1066-82 e5.
81. Nolan S, Vignali M, Klinger M, Dines JN, Kaplan IM, Svejnoha E, et al. A large-scale database of T-cell receptor beta (TCRbeta) sequences and binding associations from natural and synthetic exposure to SARS-CoV-2. *Research square.* 2020.
82. Breton G, Mendoza P, Hagglof T, Oliveira TY, Schaefer-Babajew D, Gaebler C, et al. Persistent cellular immunity to SARS-CoV-2 infection. *J Exp Med.* 2021;218(4).
83. Fischer DS, Ansari M, Wagner KI, Jarosch S, Huang Y, Mayr CH, et al. Single-cell RNA sequencing reveals ex vivo signatures of SARS-CoV-2-reactive T cells through 'reverse phenotyping'. *Nature communications.* 2021;12(1):4515.
84. Deng X, Gu W, Federman S, du Plessis L, Pybus OG, Faria NR, et al. Genomic surveillance reveals multiple introductions of SARS-CoV-2 into Northern California. *Science.* 2020;369(6503):582-7.
85. Rathe JA, Hemann EA, Eggenberger J, Li Z, Knoll ML, Stokes C, et al. SARS-CoV-2 Serologic Assays in Control and Unknown Populations Demonstrate the Necessity of Virus Neutralization Testing. *The Journal of infectious diseases.* 2021;223(7):1120-31.

86. Greaney AJ, Loes AN, Crawford KHD, Starr TN, Malone KD, Chu HY, et al. Comprehensive mapping of mutations in the SARS-CoV-2 receptor-binding domain that affect recognition by polyclonal human plasma antibodies. *Cell host & microbe.* 2021;29(3):463-76.e6.
87. Greaney AJ, Starr TN, Gilchuk P, Zost SJ, Binshtein E, Loes AN, et al. Complete Mapping of Mutations to the SARS-CoV-2 Spike Receptor-Binding Domain that Escape Antibody Recognition. *Cell host & microbe.* 2021;29(1):44-57.e9.
88. Collier DA, De Marco A, Ferreira I, Meng B, Datir RP, Walls AC, et al. Sensitivity of SARS-CoV-2 B.1.1.7 to mRNA vaccine-elicited antibodies. *Nature.* 2021;593(7857):136-41.
89. Shu Y, and McCauley J. GISAID: Global initiative on sharing all influenza data - from vision to reality. *Euro surveillance : bulletin Europeen sur les maladies transmissibles = European communicable disease bulletin.* 2017;22(13).
90. Kell A, Stoddard M, Li H, Marcotrigiano J, Shaw GM, and Gale M, Jr. Pathogen-Associated Molecular Pattern Recognition of Hepatitis C Virus Transmitted/Founder Variants by RIG-I Is Dependent on U-Core Length. *J Virol.* 2015;89(21):11056-68.
91. Esposito D, Mehalko J, Drew M, Snead K, Wall V, Taylor T, et al. Optimizing high-yield production of SARS-CoV-2 soluble spike trimers for serology assays. *Protein expression and purification.* 2020;174:105686.
92. Davies NG, Abbott S, Barnard RC, Jarvis CI, Kucharski AJ, Munday JD, et al. Estimated transmissibility and impact of SARS-CoV-2 lineage B.1.1.7 in England. *Science (New York, NY).* 2021;372(6538).
93. Voloch CM, da Silva Francisco R, Jr., de Almeida LGP, Cardoso CC, Brustolini OJ, Gerber AL, et al. Genomic characterization of a novel SARS-CoV-2 lineage from Rio de Janeiro, Brazil. *J Virol.* 2021.
94. Koelle DM. Expression cloning for the discovery of viral antigens and epitopes recognized by T-cells. *Methods.* 2003;29:213-26.
95. V'Kovski P, Kratzel A, Steiner S, Stalder H, and Thiel V. Coronavirus biology and replication: implications for SARS-CoV-2. *Nature reviews Microbiology.* 2021;19(3):155-70.
96. Koelle DM, Chen HB, Gavin MA, Wald A, Kwok WW, and Corey L. CD8 CTL from genital herpes simplex lesions: recognition of viral tegument and immediate early proteins and lysis of infected cutaneous cells. *J Immunol.* 2001;166(6):4049-58.
97. Ramirez RD, Sheridan S, Girard L, Sato M, Kim Y, Pollack J, et al. Immortalization of human bronchial epithelial cells in the absence of viral oncoproteins. *Cancer Res.* 2004;64(24):9027-34.
98. Koelle DM, Chen H, Gavin MA, Wald A, Kwok WW, and Corey L. CD8 CTL from genital herpes simplex lesions: recognition of viral tegument and immediate early proteins and lysis of infected cutaneous cells. *Journal of Immunology.* 2001;166:4049-58.
99. Johnston C, Zhu J, Jing L, Laing KJ, McClurkan CM, Klock A, et al. Virologic and immunologic evidence of multifocal genital herpes simplex virus 2 infection. *Journal of virology.* 2014;88(9):4921-31.
100. Koelle DM, Corey L, Burke RL, Eisenberg RJ, Cohen GH, Pichyangkura R, et al. Antigenic specificity of human CD4+ T cell clones recovered from recurrent genital HSV-2 lesions. *Journal of virology.* 1994;68:2803-10.
101. Yasukawa M, and Zarling JM. Autologous herpes simplex virus-infected cells are lysed by human natural killer cells. *Journal of Immunology.* 1983;131(4):2011-6.
102. Vita R, Overton JA, Greenbaum JA, Ponomarenko J, Clark JD, Cantrell JR, et al. The immune epitope database (IEDB) 3.0. *Nucleic Acids Res.* 2015;43(Database issue):D405-12.

Fig.1

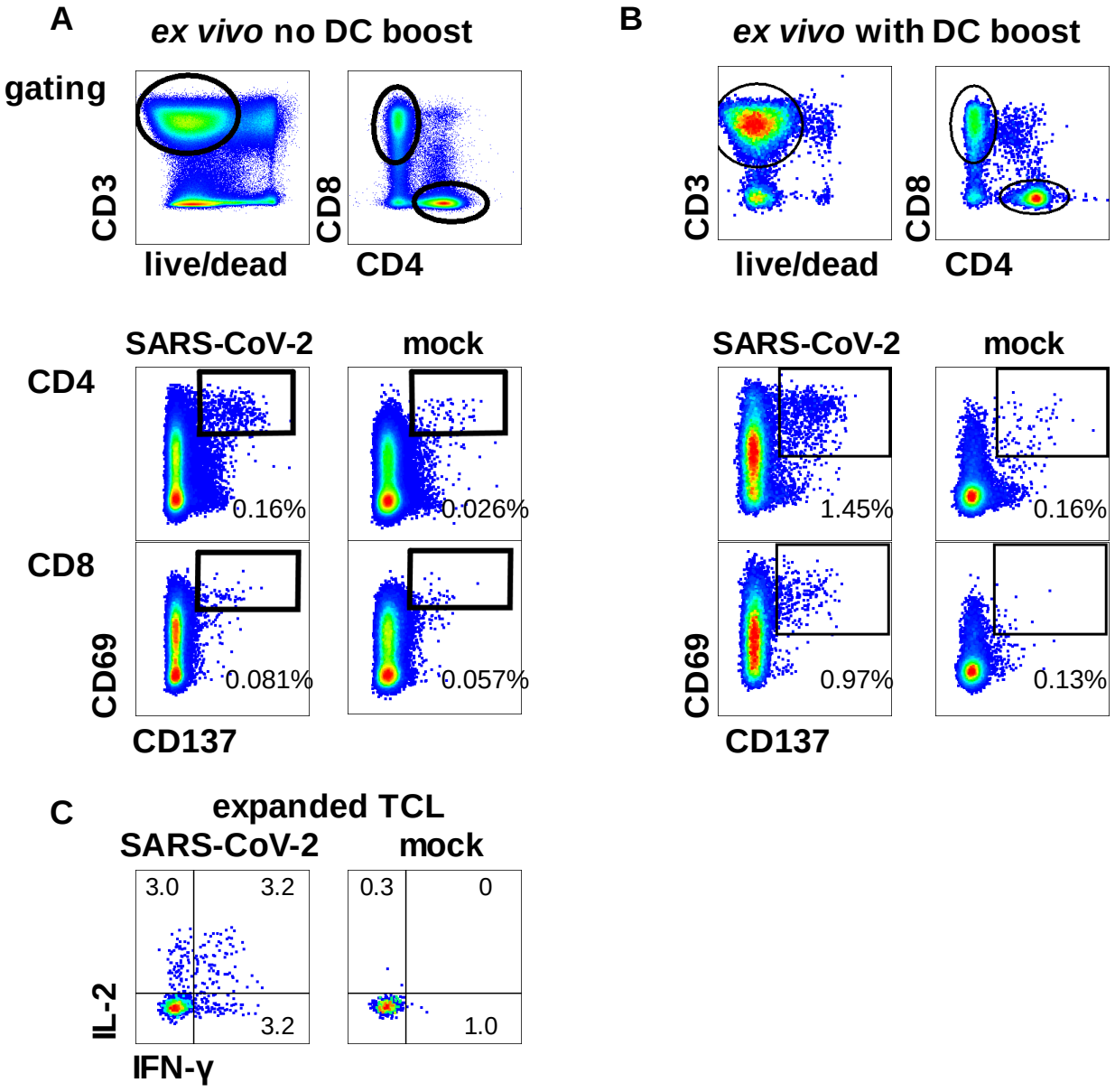

Fig. 1. AIM detection and enrichment of SARS-CoV-2 specific T cells in response to whole virus. A: PBMC from participant W003 incubated with inactivated cell-associated SARS-CoV-2 or mock antigen. Gating scheme at top. Lower panels show expression of activation markers CD137 and CD69 in response to 18 hour stimulation amongst CD4 or CD8 T cells. B: Similar layout for subject W005, specimen 1 PBMC stimulated with autologous moDC pre-treated with SARS-CoV-2 or mock antigen. Gating scheme at top. For both stimulation methods, numbers are percentages of gated T cells expressing dual activation markers. C: CD69/CD137 positive CD4 T cells from the pathway in part A: were expanded and tested for reactivity with inactivated cell-associated SARS-CoV-2 or mock antigen. Gated, live, responder, CD3+/CD4+/CD8- cells are shown. Numbers are percent of cells accumulating the indicated cytokines.

Fig.2

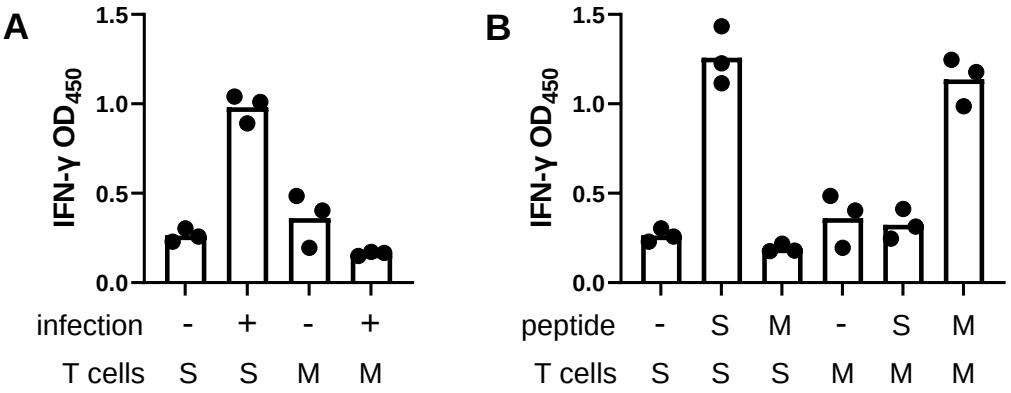

Fig. 2. Recognition of infected respiratory epithelial cells by SARS-CoV-2-specific CD8 T cells. A: HBEC3-KT-A cells with or without infection with SARS-CoV-2 were co-cultivated with tetramer-enriched, HLA A*03:01-restricted, S 378-386-specific CD8 T cells and activation measured by IFN-γ secretion. S: spike-specific T cells. M: control MCPyV-specific CD8 T cells. B: Both T cell populations specifically recognized HBEC3-KT-A cells treated with relevant viral peptide.

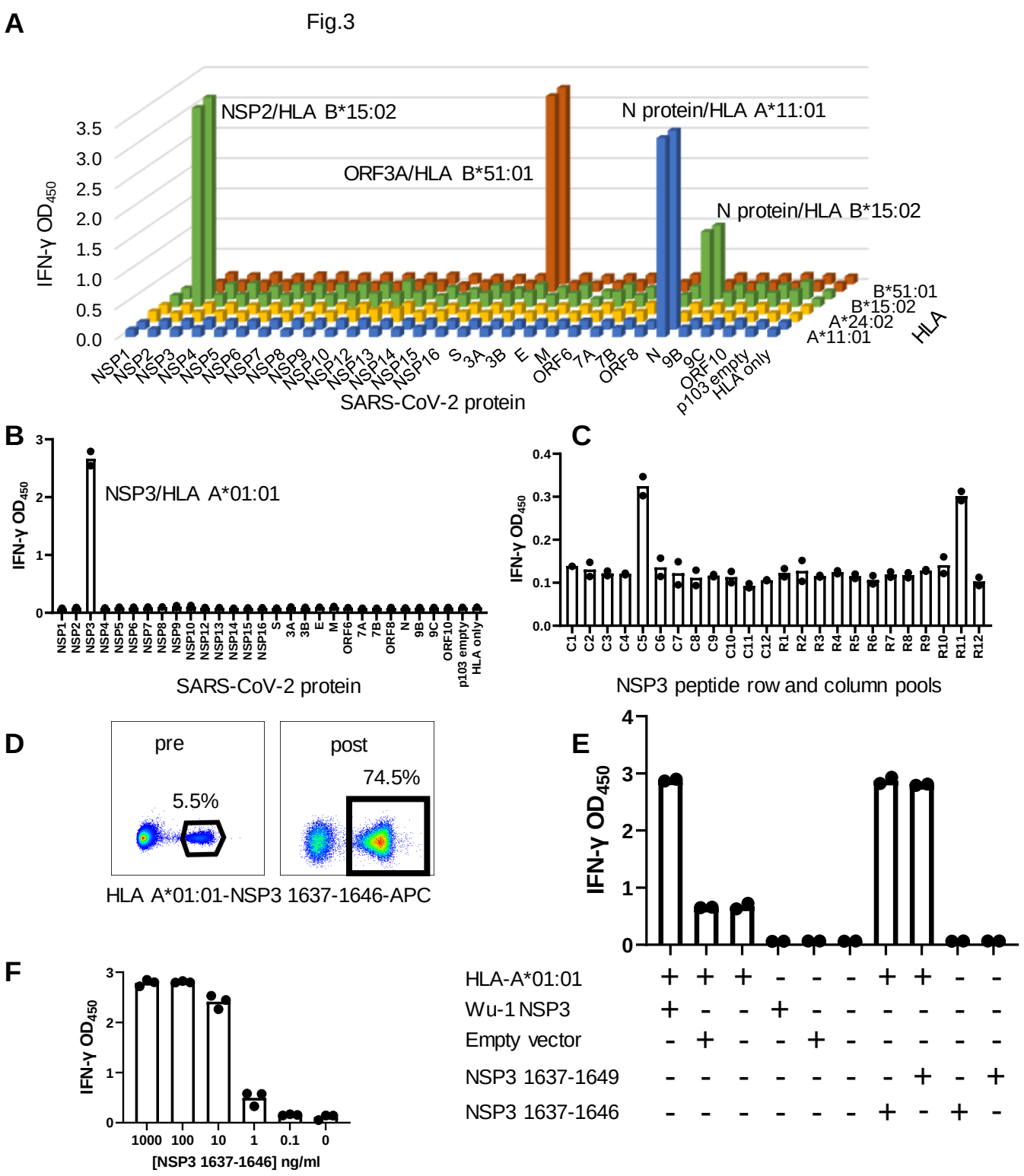

Fig. 3. SARS-CoV-2 CD8 T cell antigens and epitopes from PBMC stimulation with whole SARS-CoV-2 antigen. A: Subject W005, specimen 1 CD8 TCL were assayed with aAPC expressing each SARS-CoV-2 protein and relevant HLA A and B. Four reactivities were noted. B: Subject W010 CD8 TCL is reactive with HLA A*01:01 aAPC co-transfected with NSP3. For A: and B: negative controls at right. C: CD8 TCL from B: assayed against column (C) and row (R) pooled NSP3 peptides with autologous EBV-LCL as APC. D: Tetramer stain of CD8 TCL before and after sorting and expansion of tetramer-positive cells. Percentages of tetramer-positive cells shown E: Reactivity of tetramer-enriched cells for aAPC transfected with the indicated plasmids or treated with the indicated peptides. F: Dose-response for HLA A*01:01 aAPC with the indicated concentrations of NSP3 1637-1646. Duplicate or triplicate IFN-γ release assays show raw data as bars (A) or dots for each value and means as bars (B, C, E, F).

Fig.4

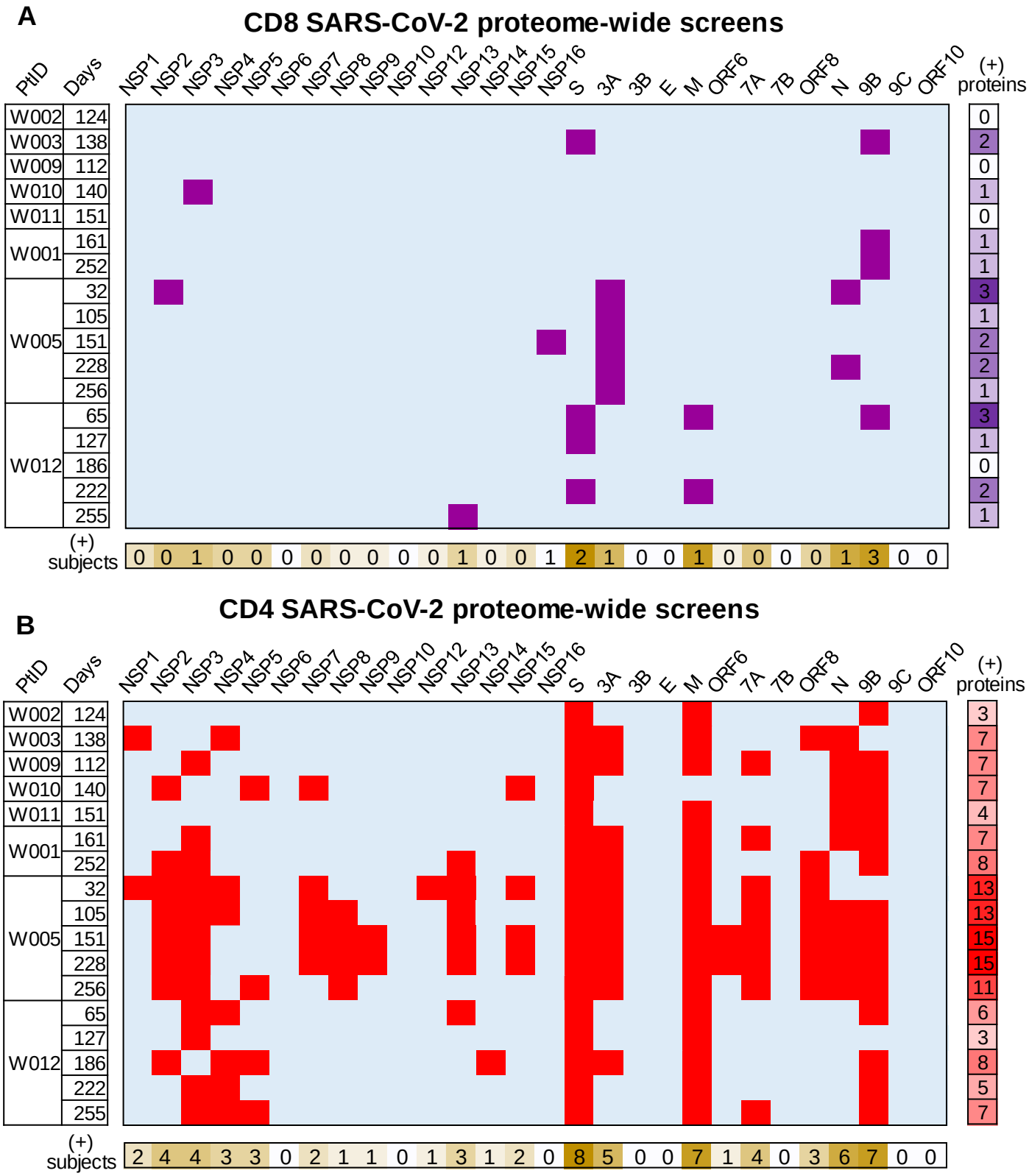

Fig. 4. Summary of SARS-CoV-2 proteome-level T cell reactivity for PBMC after COVID-19 illness, using AIM enrichment with whole viral antigen. Rows indicate donors and days between recovery from illness and PBMC sampling. Upper 5 rows were studied without DC boosting; lower 12 rows used this procedure. Columns are individual SARS-CoV-2 proteins. A: CD8 TCL scoring positive (purple). B: CD4 TCL scoring positive (red). At right are number of proteins recognized and at bottom are number of subjects with reactivity at one or more time points.

Fig.5

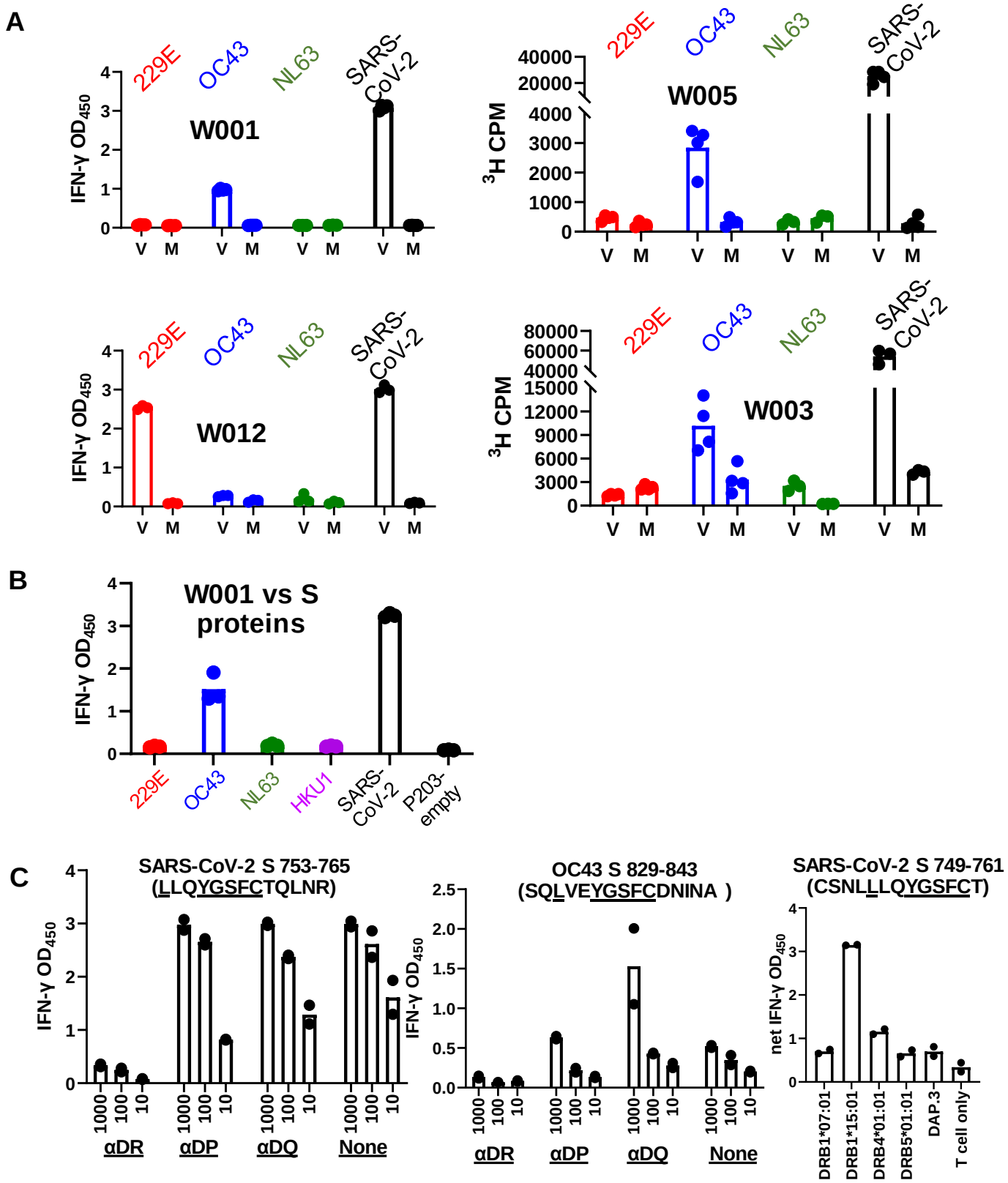

Fig. 5. A: CD4 TCL from PBMC stimulated with moDC and whole SARS-CoV-2 (subjects W001, W005, W012) or PBMC stimulated with whole SARS-CoV-2 (subject W003) recognize whole SARS-CoV-2, and sCoV OC43 or 229E antigens (V), but not mock (M) antigens. B: CD4 TCL from subject W001 recognizes full-length S protein from OC43 but not empty vector control. C: CD4 TCL recognize homologous S peptides from SARS-CoV-2 and OC43 in an HLA DR-restricted fashion as indicated by inhibition with locus-specific mAb. An overlapping SARS-CoV-2 peptide shows DRB1*15:01 restriction at right. Conserved AA are underlined.

Fig.6

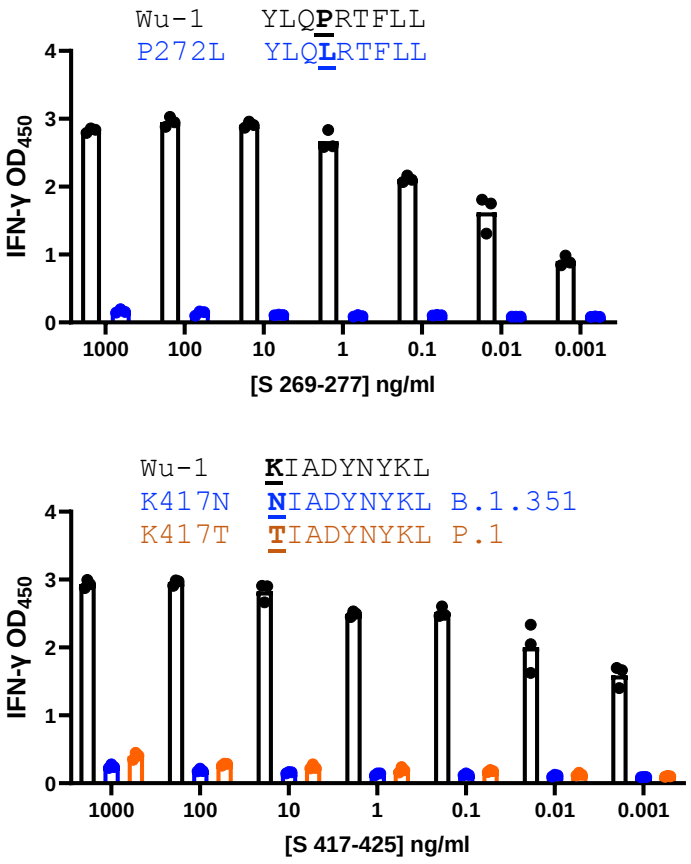

Fig. 6. CD8 TCL recognition by SARS-CoV-2 variant peptides. aAPC transfected with HLA A*02:01 and treated with wild-type but not variant peptides were recognized by polyclonal CD8 TCL lines. Lineage B.1.351 is also known as beta and P.1 is also known as gamma).

Fig. 7

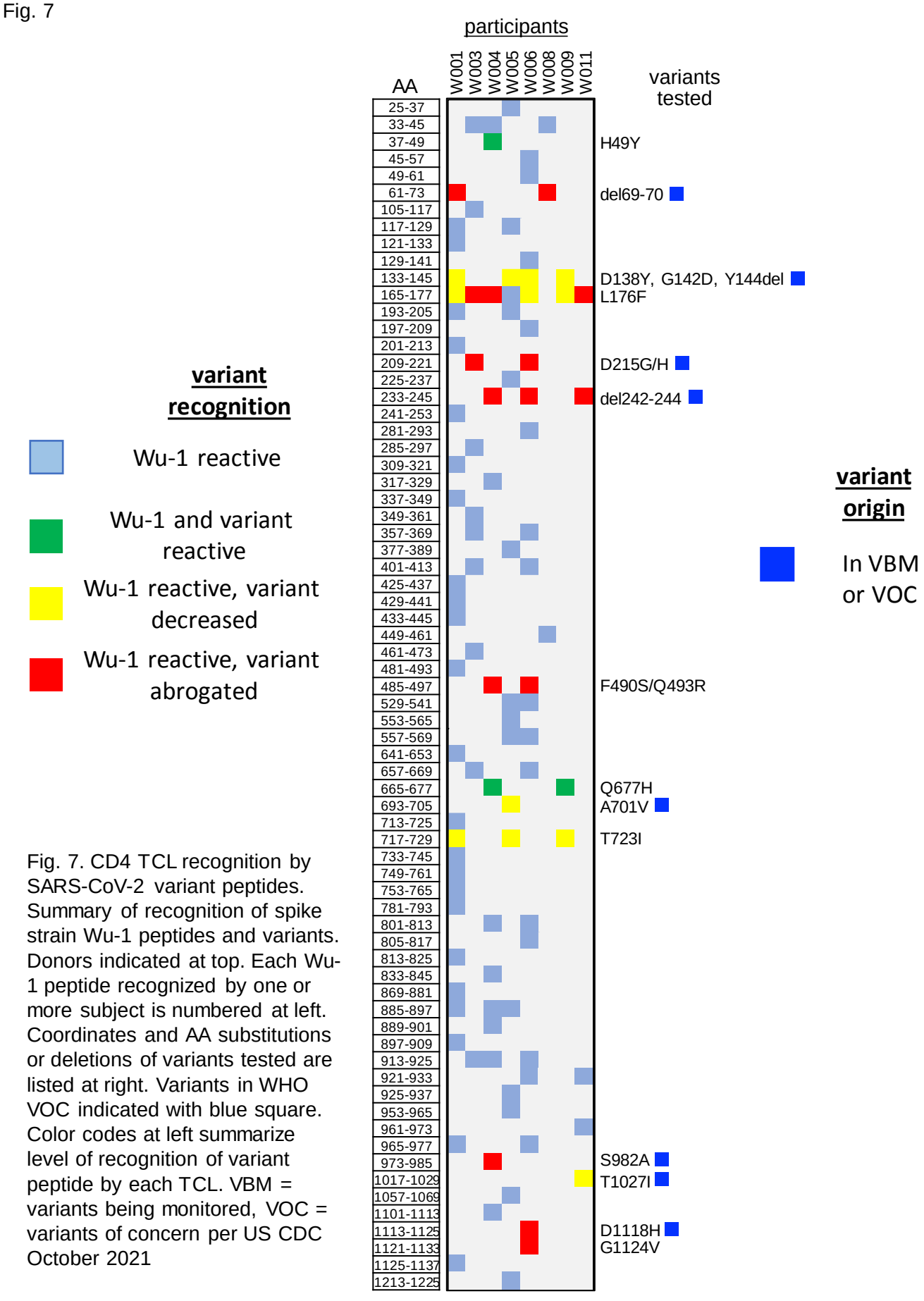

Fig. 7. CD4 TCL recognition by SARS-CoV-2 variant peptides. Summary of recognition of spike strain Wu-1 peptides and variants. Donors indicated at top. Each Wu-1 peptide recognized by one or more subject is numbered at left. Coordinates and AA substitutions or deletions of variants tested are listed at right. Variants in WHO VOC indicated with blue square. Color codes at left summarize level of recognition of variant peptide by each TCL. VBM = variants being monitored, VOC = variants of concern per US CDC October 2021